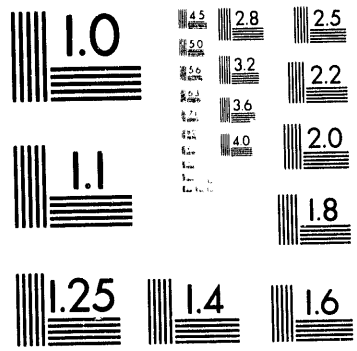
1.0
1.1
1.25
1.4
1.6
1.8
2.0
2.2
2.5
2.8
3.2
3.6
4.0
4.5
5.0

1 of 1

SAND92-7328
Unlimited Release
Printed October 1993

Distribution
Category UC-[redacted]
901,902

A Literature Review of Actinide-Carbonate Mineral Interactions

Daniel L. Stout
Department of Geological Sciences
University of Missouri-Columbia
Columbia, MO 65211, USA

Susan A. Carroll
Lawrence Livermore National Laboratory
Earth Sciences Department
Livermore, CA 94550, USA

ABSTRACT

Chemical retardation of actinides in groundwater systems is a potentially important mechanism for assessing the performance of the Waste Isolation Pilot Plant (WIPP), a U.S. Department of Energy facility intended to demonstrate safe disposal of transuranic waste. Rigorous estimation of chemical retardation during transport through the Culebra Dolomite, a water-bearing unit overlying the WIPP, requires a mechanistic understanding of chemical reactions between dissolved elements and mineral surfaces. This report represents a first step toward this goal by examining the literature for pertinent experimental studies of actinide-carbonate interactions. A summary of existing models is given, along with the types of experiments on which these models are based. Articles pertaining to research into actinide interactions with carbonate minerals are summarized. Select articles involving trace element-carbonate mineral interactions are also reviewed and may serve as templates for future research. A bibliography of related articles is included. Americium(III), and its nonradioactive analog neodymium(III), partition strongly from aqueous solutions into carbonate minerals. Recent thermodynamic, kinetic, and surface studies show that neodymium is preferentially removed from solution, forming a Nd-Ca carbonate solid solution. Neptunium(V) is rapidly removed from solution by carbonates. Plutonium incorporation into carbonates is complicated by multiple oxidation states. Little research has been done on the radium(II) and thorium(IV) carbonate systems. The removal of uranyl ion from solution by calcite is limited to monolayer surface coverage by both the large size of the uranyl species and by carbonate complexation.

FOREWORD

This document was prepared in support of the Sandia National Laboratories (SNL) research effort for the Waste Isolation Pilot Plant (WIPP). The WIPP is a U.S. Department of Energy facility intended to demonstrate the safe disposal of transuranic nuclear waste; SNL is the scientific advisor to the WIPP.

One of the current driving scenarios for WIPP performance assessment is human intrusion, where one or several boreholes are drilled into or through the waste panel(s) in the WIPP after closure and decommissioning. Under human intrusion scenarios, dissolved or colloidal actinides may be transported up a breach borehole to the Culebra Dolomite Member of the Rustler Formation, a dolomitic (calcium-magnesium carbonate) water-bearing unit overlying the WIPP Site. Should this scenario occur, actinides could be transported through the Culebra and might eventually reach the accessible environment. One potentially important mechanism for reducing this transport is chemical interaction between the actinides and the mineral phases in the Culebra, which could effectively immobilize some fraction of the actinides via incorporation into carbonate minerals, and thus reduce release from the Culebra. This report summarizes information available in the literature regarding actinide-carbonate interactions; it will serve as a preliminary guide for experimental studies for chemical retardation at the WIPP.

CONTENTS

Figures

Tables

1.0 INTRODUCTION

The geochemistry of actinides is a topic of growing scientific attention as researchers seek more rigorous and predictive chemical migration models. In order to predict the overall safety of radioactive waste disposal, it is imperative that radionuclide-mineral-water interactions be understood within a thermodynamic and kinetic framework. In the past, much research focused on the generation of empirical parameters such as distribution coefficients and kinetic data that rarely have predictive value beyond the conditions of the experiment. Future studies should include thermodynamic and kinetic experiments, as well as observations of the aqueous and solid phases, to reveal the mechanisms controlling the mobility of radionuclides in the geosphere.

This review summarizes a significant portion of the actinide-carbonate studies that are available in major geochemical journals. However, it must be noted that few studies have been carried out within a rigorous thermodynamic or kinetic framework. No attempt is made here to compare the results of the different studies. The first part of this report reviews sorption and coprecipitation models commonly applied to mineral-water interactions. The main body summarizes the various actinide-carbonate studies, concentrating on methodology, models, and results. Following the actinide reviews are a few select trace element-carbonate studies that may serve as guidelines for future research in the actinide-carbonate system. Finally, a bibliography of related actinide and trace element-carbonate studies is provided.

The literature contains a great deal of ambiguity concerning the terms sorption, absorption, adsorption, precipitation, coprecipitation, and solid solution. Sorption is a broad term that encompasses three different processes: (1) absorption that involves the diffusion of an aqueous solute into a porous solid phase; (2) adsorption that involves ions being held at a solid interface by electrostatic forces (non-specific adsorption or physisorption) and/or the chemical attraction of coordinatively unsatisfied ions at the surface (specific adsorption or chemisorption); and (3) surface precipitation, which occurs as a surface phase grows by propagation of a molecular unit that repeats itself outward into the solution. Surface precipitation may also include the formation of an ordered solid solution. Coprecipitates or solid solutions may form when a trace ion occupies structural sites within a mineral's lattice, or more rarely when the ion occupies non-lattice positions. The term coprecipitation is generally used to describe precipitation of a mixed phase from solutions supersaturated with respect to both the major and trace solid end-member components. However, solid solution development is not limited to such conditions; solid solutions may form by a number of processes, including solid-state diffusion of an adsorbed ion

into a substrate, the exchange of ions at an interface, and the incorporation of trace ions during recrystallization.

Symbols used throughout the text are listed in Table 1-1.

Table 1-1. Tabulation of Symbols Used

[i]	concentration of aqueous species i
{i}	activity of aqueous species i
γ_i	activity coefficient for aqueous species or solid component i
X_i	mole fraction of component i
X_i^*	mole fraction of component i at the mineral surface
Me	radionuclide or trace metal
Me_T	total radionuclide or trace metal
Mc	major cation (usually Ca, Mg, etc.)
Γ	moles $Me_{adsorbed}$/moles Mc
>Me	surface species Me
K_{sp}	solubility product
K_D	distribution coefficient
D	homogenous partition coefficient
λ	logarithmic partition coefficient
K_{ex}	thermodynamic exchange constant
${}^cK_{ex}$	conditional exchange constant
K_{ex}^*	thermodynamic surface exchange constant
K_{ads}	adsorption constant
S_T	total available surface sites
DI	distilled and/or deionized water
SW/ASW	sea water / artificial sea water
GW/AGW	ground water / artificial ground water
AES	Auger electron spectroscopy
BEI	backscattered electron imagery
EDS	energy dispersive spectroscopy
LEED	low energy electron diffraction
RBS	Rutherford backscattering spectroscopy
SEM	scanning electron microscopy
XPS	X-ray photoelectron spectroscopy

2.0 MODELS

2.1 The Distribution Coefficient (K_D) Model

Until the early 1980s, sorption modeling focused on the generation of empirical distribution coefficients, K_D, defined as:

$$K_D = \frac{[Me]_{solid}}{[Me]_{solution}} \quad (1)$$

where [Me] represents the trace element concentration in the solid or solution phase. K_D values are highly conditional upon pH, mineralogy, available surface area, free metal concentrations, and complexing ligands (see for example Novak, 1992). Thus, the distribution coefficient effectively describes only the experiment from which it is derived. Little information for discriminating the processes at work (e.g., precipitation, adsorption, diffusion) may be assessed, and predictive value is minimal. Unless otherwise specified, K_D values reported in this review are dimensionless.

2.2 The Homogeneous Partition Coefficient (D) Model

If a solid phase (a pure solid or a solid solution) is homogeneous and in equilibrium with an aqueous phase, the partitioning of the components between the two phases defines the homogeneous or Berthelot-Nernst partition coefficient, D, which is defined by McIntire (1963) as:

$$D = \frac{\left(\frac{[Me]}{[Mc]}\right)_{solid}}{\left(\frac{[Me]}{[Mc]}\right)_{solution}} \quad (2)$$

The numerator is the concentration ratio of the trace component (Me) to the major component (Mc) in the solid phase, and the denominator is the same ratio for the accompanying solution. D is a dimensionless quantity. The homogeneous partition coefficient has generally been used to describe coprecipitation. If D is greater than unity, the precipitate is enriched in the trace component relative to the solution. However, several investigators have shown that the distribution of trace elements in carbonates is controlled by kinetic reactions (see for example Davis et al., 1987; Franklin and Morse, 1982; Lorens, 1981; McBride, 1979; Pingitore, 1986). Therefore, the partition coefficient is generally not a thermodynamic constant and will vary with changes in the composition of the system.

2.3 The Logarithmic Partition Coefficient (λ) Model

The Doerner-Hoskins, or logarithmic partition coefficient, λ, is defined as:

$$\lambda = \frac{\log\left(\frac{[Me]_i}{[Me]_f}\right)}{\log\left(\frac{[Mc]_i}{[Mc]_f}\right)} \tag{3}$$

where the numerator and denominator are the log ratios of the initial and final aqueous concentrations of the trace and major elements, respectively (McIntire, 1963). As the solution composition changes during precipitation, a heterogeneous distribution of the trace component occurs in the solid phase. Solid-state diffusion is generally regarded as too slow to maintain equilibrium between the interior of the crystal and the aqueous phase at earth-surface temperatures and pressures. The rate of crystallization, and hence the degree of supersaturation, affects the observed value of λ. Like the homogeneous partition coefficient, the logarithmic partition coefficient is not a thermodynamic constant and will vary with changes in the system.

2.4 Exchange Model

The exchange model is founded on the thermodynamics of both the aqueous and solid phases. Regardless of the mechanism of solid solution formation, the system may be defined in terms of the activities of the components. If a solid solution is in equilibrium with an aqueous phase, the exchange of cations between the solid (using calcium carbonate, for example) and the aqueous phase may be described as:

$$Me^{2+} + CaCO_3(s) \leftrightarrow MeCO_3(s) + Ca^{2+} \tag{4}$$

The corresponding thermodynamic exchange constant is defined as:

$$K_{ex} = \frac{\{MeCO_3(s)\}\{Ca^{2+}\}}{\{CaCO_3(s)\}\{Me^{2+}\}} \tag{5}$$

K_{ex} is equal to the ratio of the pure end-member solubility products:

$$K_{ex} = \frac{K_{sp}(CaCO_3(s))}{K_{sp}(MeCO_3(s))} \tag{6}$$

where $K_{sp}(CaCO_3(s))$ and $K_{sp}(MeCO_3(s))$ are given by:

$$K_{sp}(CaCO_3(s)) = \frac{\{Ca^{2+}\}\{CO_3^{2-}\}}{\{CaCO_3(s)\}} \quad (7)$$

$$K_{sp}(MeCO_3(s)) = \frac{\{Me^{2+}\}\{CO_3^{2-}\}}{\{MeCO_3(s)\}} \quad (8)$$

for the reactions:

$$CaCO_{3(s)} \leftrightarrow Ca^{2+} + CO_3^{2-} \quad (9)$$

$$MeCO_{3(s)} \leftrightarrow Me^{2+} + CO_3^{2-} \quad (10)$$

The ratio of Equations 7 and 8 yields Equation 6. If the solid solution is ideal (i.e., activity coefficients of the solid components are unity) K_{ex} may be expressed by the equation:

$$K_{ex} = IAP \frac{X_{Me}}{X_{Ca}} \quad (11)$$

where IAP represents the ion-activity product of the solution and X_{Me} and X_{Ca} are the mole fractions of the trace element and Ca in the solid. If the solid solution exhibits non-ideal behavior, activity coefficients of the solid trace and major elements, γ_i, must be taken into account, and Equation 11 becomes:

$$K_{ex} = IAP \frac{X_{Me}\gamma_{Me}}{X_{Ca}\gamma_{Ca}} \quad (12)$$

2.5 The Surface Precipitation Model

Ions specifically adsorbed to a substrate have a tendency to form an insoluble compound with an ion of opposite charge on that surface. As more adsorbate is added, a solid component forms. A model describing the transition from adsorption to surface precipitation onto metal oxides was derived by Farley et al. (1985). Comans and Middelburg (1987) and Wersin et al. (1989) have applied this surface precipitation model to the carbonate mineral system. Three independent reactions and their corresponding equilibrium constants describe the trace metal-calcite system. The first two reactions represent the coprecipitation of $CaCO_3$-$MeCO_3$:

$$Ca^{2+} + CO_3^{2-} \leftrightarrow CaCO_3(s) \quad (13)$$

$$Me^{2+} + CO_3^{2-} \leftrightarrow MeCO_3(s) \tag{14}$$

with their respective equilibrium solubility product expressions:

$$K_{sp}(CaCO_3(s)) = \frac{\{Ca^{2+}\}\{CO_3^{2-}\}}{\{CaCO_3(s)\}} \tag{15}$$

$$K_{sp}(MeCO_3(s)) = \frac{\{Me^{2+}\}\{CO_3^{2-}\}}{\{MeCO_3(s)\}} \tag{16}$$

Equation 17 represents the adsorption of Me^{2+} at a calcite surface site, indicated by the > symbol here:

$$>CaCO_3 + Me^{2+} + CO_3^{2-} \leftrightarrow CaCO_3(s) + >MeCO_3 \tag{17}$$

and may be described with the adsorption constant:

$$K_{ads} = \frac{\{CaCO_3(s)\}[>MeCO_3]}{[>CaCO_3]\{Me^{2+}\}\{CO_3^{2-}\}} \tag{18}$$

The adsorption of Me^{2+} in Equation 17 creates a new surface site and the underlying $CaCO_3$ is incorporated into the bulk solid. The adsorption of Ca^{2+} onto $MeCO_3(s)$ may be represented by a combination of the three reactions resulting in a thermodynamic equilibrium constant equal to

$$\frac{1}{K_{ads}\, K_{sp}(CaCO_3(s))\, K_{sp}(MeCO_3(s))} \tag{19}$$

The mass balance equations for the total Me concentration (Me_T), total Ca concentration (Ca_T), and the total surface reaction sites (S_T) may be written as:

$$Me_T = [Me^{2+}] + [>MeCO_3] + [MeCO_3(s)] \tag{20}$$

$$Ca_T = [Ca^{2+}] + [>CaCO_3] + [CaCO_3(s)] \tag{21}$$

$$S_T = [>CaCO_3] + [>MeCO_3] \tag{22}$$

The conditional equilibrium constant, ${}^cK_{ads}$, may be obtained from the low concentration-surface coverage portion of the sorption isotherms shown in Figure 2-1 (Farley et al., 1985). Sorption isotherms typically exhibit an inflection point assumed to represent the saturation of surface sites,

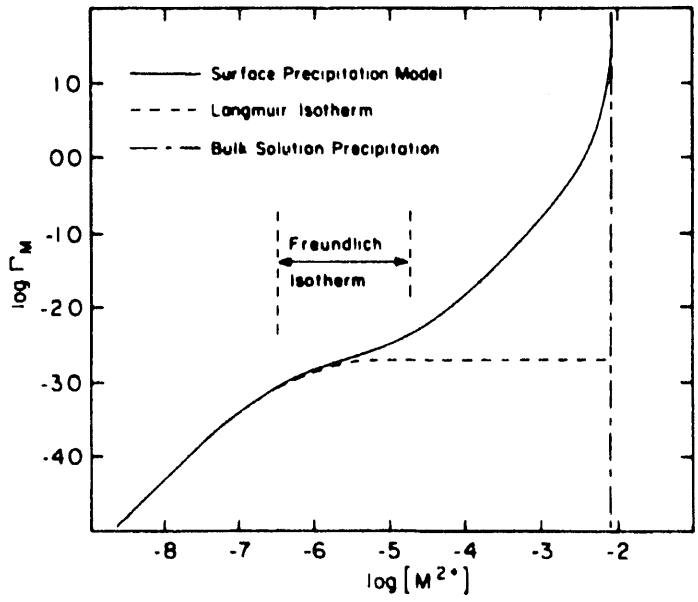

Figure 2-1. Sorption isotherm behavior for the surface precipitation model (Farley et al., 1985).

allowing estimation of S_T. The surface precipitation model predicts a smooth transition from adsorption to surface precipitation with increasing Me concentration. A line asymptotic to low concentration data represents adsorption far from saturation where:

$$\Gamma_{Me} \approx \frac{[>MeCO_3]}{Ca_T} \tag{23}$$

Integration of the above equations allows calculation of the amount of Me^{2+} sorbed at any equilibrium Me^{2+} concentration, Γ_{Me}, to be expressed by:

$$\Gamma_{Me} = {}^{c}K_{ads} \frac{S_T}{Ca_T} \frac{[HCO_3^-]}{[H^+]} [Me^{2+}] \tag{24}$$

A major limitation of this model is its assumption that the sorption processes are at equilibrium. Numerous studies have shown that the kinetics of reaction control the concentration of trace elements in carbonate phases (see for example Davis et al., 1987; Franklin and Morse, 1982; Lorens, 1981; McBride, 1979; Pingitore, 1986). Also, the surface precipitation model assumes a solid solution forms only after available adsorption surface sites have been saturated. Other research has shown that this is not the case; solid solutions can form at low surface loadings (Davis et al., 1987; Stipp et al., 1992; Zachara et al., 1991).

2.6 Dynamic Feedback

Wang and Merino (1992) explain oscillatory zoning of trace elements in calcite as a result of an electrostatic feedback mechanism. Calcite growth releases H^+, which accumulates at the calcite surface if growth is rapid enough. The buildup of positive charges repels adsorbing trace cations, and calcite growth accelerates due to the high Ca^{2+} chemical potential. Eventually, depletion of Ca^{2+} in the interfacial region occurs, slowing production of H^+, and trace cations adsorb again. The possibility that trace element zoning in calcite results from the dynamics of growth makes it unnecessary to interpret oscillatory zoning in terms of drastic changes in solution composition. While the dynamic feedback model offers an explanation for the observed oscillatory zoning of trace elements, it has not been tested with experimental data.

3.0 ACTINIDES

A summary of reviewed actinide-carbonate mineral research is provided in Table 3-1.

Table 3-1. Summary of Reviewed Actinide-Carbonate Mineral Research

Author	Sorbate	Sorbent	Background solution	Experiment type	Value	Comments
Shanbhag and Morse (1982)	Am(III)	calcite aragonite biogenic carb.	DI, 0.7M NaCl- $MgCl_2$, ASW, SW	kinetic distribution	$K_D = 10^{5.30}$	$[Am]=10^{-8.48}$ M
Higgo and Rees (1986)	Am(III)	65% calcite sediment	SW	distribution	$K_D = 10^{6.0}$	all [Am] and S/S ratios
Allard (1984)	Am(III)	calcite	AGW 4M NaCl	distribution	$K_D = 10^{3.85}$ $K_D = 10^{4.47}$	pH 6.5 pH 9.0
Dosch (1979)	Am(III)	dolomite	AGW NaCl brine	distribution	$K_D = 10^{4.34}$ $K_D = 10^{3.41}$	AGW NaCl brine
Dosch and Lynch (1980)	Am(III)	dolomite, proto-dolomite	AGW	distribution	$K_D = 10^{3.30}$ to $10^{4.30}$	n/a
Carroll (1993)	Nd(III)	calcite aragonite	$NaHCO_3$	exchange kinetic surface	$Kex = 10^{0.84}$ $Kex = 10^{0.52}$	$[Nd] \geq 10^{-4.5}$M $[Nd] \leq 10^{-5.5}$M
Carroll et al. (1992)	Nd(III)	calcite	$NaHCO_3$	surface	n/a	SEM, BEI, EDS
Mecherri et al. (1990)	Nd(III)	calcite	DI	kinetic distribution	$K_D = 10^{3.38}$	$[Nd]=10^{-5.48}$M
Keeney-Kennicutt and Morse (1984)	NpO_2^+	calcite aragonite carb. sediment	DI, 0.7M NaCl- $MgCl_2$, ASW, SW	kinetic	n/a	n/a
Higgo and Rees (1986)	Np(V)	65% calcite sediment	SW	distribution	$K_D = 10^{3.60}$	$[Np]=10^{-7.47}$M all S/S ratios
Allard (1984)	Np(V)	calcite	AGW 4M NaCl	distribution	$K_D < 10^{2.3}$ $K_D = 10^{3.60}$	pH 6.5 pH 9.0
Ames and Rai (1978)	Np(V)	calcite	n/a	distribution	$K_D = 10^{3.70}$	n/a
Higgo and Rees (1986)	Pu	65% carbonate sediment	SW	distribution	$K_D = 10^{2\text{-}2.3}$ $K_D > 10^4$	high S/S ratios low S/S ratios
Gromov & Spitsyn (1974)	Pu	carbonate sediment	SW	distribution	$K_D = 10^{4.04}$	n/a
Ginzburg and Maksimov (1975)	Pu(IV)	carbonate precipitates	DI	partition	n/a	n/a
Dosch (1979)	Pu	dolomite	AGW NaCl brine	distribution	$K_D = 10^{3.86}$ $K_D = 10^{3.32}$	AGW NaCl brine
Dosch and Lynch (1980)	Pu	dolomite proto-dolomite	AGW	distribution	$K_D = 10^{3.30}$ to $10^{3.85}$	n/a

Table 3-1. Summary of Reviewed Actinide-Carbonate Mineral Research (continued)

Author	Sorbate	Sorbent	Background solution	Experiment type	Value	Comments
Gnanapragasam (1991)	Ra	carbonate precipitates	DI	partition	$1 = 10^{-1.89}$	$Ra^{2+}/Ca^{2+} = 10^{-6}$ to 10^{-9}
Carroll et al. (1992)	Th	calcite	$NaHCO_3$	surface	n/a	SEM, BEI
Carroll and Bruno (1991)	U(VI)	calcite	$NaHCO_3$	kinetic exchange	$K^*_{ex} = 10^{-5.12\pm0.53}$	n/a
Carroll et al. (1992)	U(VI)	calcite	$NaHCO_3$	surface	n/a	SEM, BEI, RBS
Morse et al. (1984)	U(VI)	calcite aragonite biogenic carb.	DI SW	kinetic	n/a	n/a
Milton and Brown (1987)	U(VI)	calcite	GW	kinetic	n/a	n/a
Kitano and Oomori (1971)	U(VI)	Mg-calcite aragonite	$Ca(HCO_3)_2$	partition	$1 = 10^{-2}$ to -0.7 $= 10^{-0.52}$ to 0	calcite aragonite

3.1 Americium (Am) and Neodymium (Nd)

Neodymium, commonly used as a chemical analog for americium, is included in this section.

Carroll (1993) studied the thermodynamics and kinetics of Nd-Ca carbonate solid-solution formation. Three different types of kinetic experiments investigated the formation of a Nd-Ca carbonate solid solution. The first set of experiments investigated the effects of initial aqueous Nd concentrations on solid solution kinetics. The second set explored the formation of a solid solution from near-saturation by reacting a Nd-carbonate with calcite. The third set studied the formation of a solid solution from a solution saturated with respect to $NdOHCO_3(s)$ and undersaturated with respect to calcite or aragonite. Batch reaction techniques were used for all three experiment types, and reaction times varied between 30 and 40 days.

The Nd-Ca-CO_2-H_2O system is somewhat unique in that Nd^{3+} has a smaller ionic radius and higher valence than Ca^{2+}, and the solid solution occurs in the precipitated trace element phase rather than in the major phase. Aqueous Ca^{2+} and Nd^{3+} concentrations were controlled by the precipitation of a homogeneous Nd-Ca solid solution from the bulk solution. The solid solution, as shown by the experimental results, was more stable (i.e., less soluble) than its pure end-member components. Two distinct Nd-rich morphologies were observed with scanning electron microscopy (SEM) and backscattered electron imagery (BEI): a submicron fibrous precipitate, and larger bladed crystals. Energy dispersive spectroscopy (EDS) analyses of the larger bladed

crystals indicated that the Nd-rich carbonate phases were homo-geneous solid solutions containing approximately eight mole-percent calcium. The solid solution was interpreted to be orthorhombic, as orthorhombic $NdOHCO_3(s)$, the stable Nd-carbonate phase in the absence of Ca, and Ca^{2+} substituted for Nd^{3+} in the precipitated trace element phase. In all likelihood, the bladed crystals formed by Ostwald ripening (Parks, 1990) at the expense of the small Nd-rich fibrous crystals.

The Nd-Ca carbonate phase was modeled as a solid solution between aragonite and $NdOHCO_3(s)$, both of which have orthorhombic structures. The development of the solid solution may be described by the exchange reaction:

$$CaCO_3(s) + Nd^{3+} + H_2O \leftrightarrow NdOHCO_3(s) + Ca^{2+} + H^+ \quad (25)$$

and the corresponding equilibrium exchange constant, K_{ex}:

$$K_{ex} = \frac{\{NdOHCO_3(s)\}\{Ca^{2+}\}\{H^+\}}{\{CaCO_3(s)\}\{Nd^{3+}\}} \quad (26)$$

The exchange reaction equilibrium constant is also equal to the ratio of the pure end-members' solubility products:

$$K_{ex} = \frac{K_{sp}(\text{aragonite})}{K_{sp}(NdOHCO_3(s))} \quad (27)$$

where:

$$K_{sp}(\text{aragonite}) = \frac{\{Ca^{2+}\}\, pCO_2(g)}{\{H^+\}^2\, \{CaCO_3(s)\}} \quad (28)$$

$$K_{sp}(NdOHCO_3(s)) = \frac{\{Nd^{3+}\}\, pCO_2(g)}{\{H^+\}^3\{\, NdOHCO_3(s)\}} \quad (29)$$

for the reactions:

$$CaCO_3(s) + 2H^+ \leftrightarrow Ca^{2+} + CO_2(g) + H_2O \quad (30)$$

$$NdOHCO_3(s) + 3H^+ \leftrightarrow Nd^{3+} + CO_2(g) + 2H_2O \quad (31)$$

respectively. K_{ex} equals $10^{-0.60}$ for an orthorhombic $NdOHCO_3(s)$ and aragonite solid solution.

The solution compositions reached a steady state within 200 hours of reaction, but they did not reach equilibrium. The solid solution was non-ideal, as the substitution of Ca^{2+} for Nd^{3+} into orthorhombic $NdOHCO_3(s)$ resulted in a reduction of the unit-cell volume. It was not

possible to determine the activity of the solid components; therefore, only conditional constants were calculated from the steady-state solution compositions. The conditional constant, defined as

$$^{c}K_{ex} = \frac{\{Ca^{2+}\}\{H^{+}\}}{\{Nd^{3+}\}} \quad (32)$$

equals the IAP of reaction 25. The constant $^{c}K_{ex}$ equaled $10^{0.84}$ and $10^{0.52}$ for initial Nd^{3+} concentrations greater than or equal to $10^{-4.5}$ M and less than or equal to $10^{-5.5}$ M, respectively. The conditional constant represents an upper limit for aqueous concentrations of Nd. Similar values would be expected for Am(III).

Carroll et al. (1992) examined Nd(III)-calcite surface interactions with SEM, BEI, and EDS at 50°C. Initial Nd^{3+} concentrations were below 10^{-3} M in a background solution of $10^{-2.30}$ M of $NaHCO_3$. At initial Nd concentrations of $10^{-5.72}$ M, small fibrous Nd-rich crystals approximately 20 μm in length precipitated at the calcite surface. At the moment the experiment was terminated, the calcite appeared to be reacting with the Nd-rich crystals, implying that the system had not reached equilibrium. At higher Nd concentrations, both fibrous and euhedral star-shaped crystals were observed on the calcite surface. The core and inner arms of the star-shaped crystals were Nd-rich and increasingly Ca-rich outward. Based on the BEI image and EDS analysis, it was clear that a Nd-Ca carbonate solid solution had formed.

Smith (1990) modeled Am(III) substitution into calcite based on lattice energy considerations. In order for substitution of the trivalent cation to occur, two Am^{3+} cations may substitute for three Ca^{2+} in the solid phase. The results of these calculations are that americium substitution in calcite is highly non-ideal and that very limited substitution is likely.

Shanbhag and Morse (1982) investigated the interactions of Am(III) with calcite and aragonite and stipulated that Am(III) may be used as a representative element for all trivalent actinides. Initial Am^{3+} concentrations ranged from 10^{-12} to 10^{-7} M. Background solutions included deionized water, 0.7 M NaCl, a 0.7 M NaCl-$MgCl_2$ solution, and both artificial and natural sea waters equilibrated with either calcite or aragonite. All experiments were conducted at atmospheric $CO_2(g)$ pressure. Mineral surface areas were taken into consideration, and solid/solution ratios varied from 0.1 to 10 g/l. Mineral phases used were synthetic calcite and aragonite, three biogenic carbonates, and a natural carbonate sediment roughly characterized as a 50/50 mix of biogenic aragonite and Mg-calcite.

Preliminary experiments indicated that 99% of the initial Am^{3+} was removed from solution within a few minutes to hours. Desorption experiments involved dilution of the above suspensions with Am-free solutions. Less than one percent desorption of previously sorbed Am^{3+} was measured. The rate of Am^{3+} adsorption was directly proportional to the initial dissolved Am^{3+} concentration: at higher concentrations faster rates were observed. Am^{3+} sorption rates were not directly proportional to the solid/solution ratio, but they approximately followed the square root of the surface area-to-volume ratio.

The effect of Am^{3+} surface concentration on the extent of adsorption was determined using ten successive spikes of Am^{3+} added at 30-minute intervals. A total addition of $10^{-8.15}$ M of Am^{+3} was added to a 5 g/l calcite suspension. The extent of adsorption after each addition was 99% within 30 minutes. Thus, over the concentrations studied, there was no measurable influence of surface concentration on the extent of adsorption. This behavior indicated that equivalent reactive surface sites either were not saturated or that an americium phase precipitated.

Adsorption rates onto aragonite were 40 times faster than onto calcite when normalized for surface area. Experiments at similar Am^{3+} concentrations and solid/solution ratios including NaCl and/or $MgCl_2$ indicated that epitaxial differences accounted for 15% of the increased rate, whereas the presence of Mg^{2+} accounted for the remaining 85% of the adsorptive difference between calcite and aragonite in sea water.

Because of the microporous nature of biogenic carbonates, representative surface area characterization was not possible. On a mass basis, the adsorption rate of biogenic Mg-calcites and the calcareous sediment agreed well with that of the synthetic calcites. In contrast, adsorption onto synthetic aragonite was approximately 100 times faster than onto biogenic aragonite.

A K_D of $10^{5.30}$ was determined for an initial Am^{3+} concentration of $10^{-8.48}$ M and a solid/solution ratio of 5 g/l. This K_D value, obtained at a very low concentration and solid/solution ratio, was the lowest determined by this experimental methodology.

Mecherri et al. (1990) conducted a limited study of the interactions of Nd(III) with calcite. Batch experiments at 50°C used a solid/solution ratio of 6.67 g/l. Reaction times varied from five minutes to several weeks. Surface area was determined both optically and by BET gas adsorption.

Sorption increased with increased Nd^{3+} concentration in solution, to a limiting value of approximately $10^{-4.42}$ eq/m^2. The sorption was described by a modified distribution coefficient:

$$K_D = \left(\frac{[Nd^{3+}]_{sorbed}}{[Nd^{3+}]_{solution}} \right)^n \quad (33)$$

where n = 0.414. A value of n < 1 indicated that sorption affinity was not homogeneous and that affinity decreased with increasing surface saturation. A K_D of $10^{3.38}$ (12 l/m^2) was determined for an initial Nd^{3+} concentration of $10^{-6.48}$ M. Desorption experiments in which the reacted solid was exposed to fresh deionized water were conducted for three hours. The extent of desorption was always below 1% of the previously sorbed Nd.

Higgo and Rees (1986) examined Am(III) sorption from natural sea water on a calcareous sediment (65% calcite, 35% clays) at 4°C. Initial Am^{3+} concentrations were 10^{-10} M, and solid/solution ratios ranged from 1 to 600 g/l. A K_D of approximately 10^6 was determined at all solid/solution ratios. At high solid/solution ratios, desorption K_D values were higher than sorption K_D values, indicating that a nonsorbing phase existed in the initial sorption procedure.

Allard (1984) examined Am(III) sorption on a variety of minerals, including an uncharacterized calcite. Initial Am^{3+} concentrations ranged from $10^{-8.30}$ to $10^{-8.74}$ M. Batch experiments used equilibrated artificial ground water (AGW) and 4 M NaCl solutions. Solid/solution ratios ranged from 6 to 15 g/l. K_D values for Am(III) ranged from $10^{3.85}$ at pH 6.5 to $10^{4.47}$ at pH 9. At pH 5, K_D values were higher in the AGW than in the NaCl solution, but at pH 8 any ionic-strength or salt effects were inconclusive.

Dosch (1979) reported a K_D value for Am(III) sorption onto dolomite of $10^{4.34}$ from AGW and $10^{3.41}$ from a halite brine. Dosch and Lynch (1980) reported K_D values ranging from $10^{3.30}$ to $10^{4.30}$ for Am(III) sorption onto natural dolomite and protodolomites.

3.2 Curium (Cm)

Dosch (1979) studied Cm(III) sorption on natural dolomite and reported K_D values of $10^{5.04}$ from AGW and $10^{4.08}$ from a saturated halite brine. Reaction time was 170 days and near-neutral pH was maintained.

3.3 Neptunium (Np)

Keeney-Kennicutt and Morse (1984) demonstrated that significant adsorption of NpO_2^+ occurs on common carbonate minerals. Because of the relatively short half-life of available Np isotopes, sorption experiments were limited to two days maximum. Solid phases used were synthetic calcite, aragonite, and a natural carbonate sediment containing 15 weight-percent organic material. Initial NpO_2^+ concentrations ranged from 10^{-13} to 10^{-4} M. Background solutions included deionized water, 0.7 M NaCl, a mixed 0.7 M NaCl-$MgCl_2$ solution, and both artificial and natural sea waters with 35% salinity.

The results of this study indicated a more complex behavior of NpO_2^+ than previously thought, and a strong affinity for carbonate surfaces. A variety of factors influenced NpO_2^+ uptake, including the solid's surface characteristics, solution composition, solid/solution ratio, and time of reaction. Adsorption was rapid in all carbonate suspensions. Maximum adsorption occurred within 30 minutes at all initial NpO_2^+ concentrations and solid/solution ratios. At initial NpO_2^+ concentrations below 10^{-7} M, all carbonate minerals exhibited similar adsorptive tendencies and greater than 80% removal from solution. At higher NpO_2^+ concentrations, the maximum extent of adsorption dropped rapidly until at approximately 10^{-4} M neptunium, solubility limitations were surpassed and precipitation occurred.

At NpO_2^+ concentrations below 10^{-6} M, the rate of adsorption in sea water was significantly slower than in deionized water. In addition, natural sediment adsorbed much more slowly than synthetic aragonite, although the extent of adsorption was very similar. The maximum extent of adsorption on aragonite was slightly greater than on calcite, and adsorption from deionized water was greater than from sea water. The extent of NpO_2^+ adsorption as a function of mineralogy varied most in deionized water at low solid/solution ratios. At higher solid/solution ratios in distilled water, or at any solid/solution ratio in sea water, little difference existed between the extent of adsorption by calcite and aragonite. Desorption experiments exposed aragonite to NpO_2^+ for two hours, after which the supernatant was withdrawn and replaced with an unspiked solution. An initial desorption of 1 to 8% of previously sorbed NpO_2^+ occurred within one hour; however, most of the NpO_2^+ was resorbed onto the substrate, resulting in little net desorption.

Higgo and Rees (1986) examined the distribution of Np(V) between a calcareous sediment and sea water. The initial Np concentration was held constant at $10^{-7.47}$ M and the solid/solution ratio

was varied. After a desired reaction time, the suspensions were separated and fresh, unspiked sea water was added to the original sediment to assess desorption characteristics. The sorption of neptunium did not change with varied solid/solution ratios; it yielded a K_D value of approximately $10^{3.60}$. Desorption K_D values were approximately the same.

Allard (1984) studied Np(V) sorption on a variety of minerals, including an uncharacterized calcite. Batch experiments used equilibrated AGW and 4 M NaCl solutions. Solid/solution ratios ranged from 6 to 15 g/l, initial Np concentrations were approximately 10^{-11} M, and exposure time was 5 days. K_D values less than $10^{2.3}$ were found below pH 7.5. With increasing pH, K_D values steadily increased, reaching approximately $10^{3.60}$ at pH 9. Lower K_D values occurred in the AGW than in the NaCl solutions at pH 8, but at pH 5 any salt or ionic strength effects were inconclusive.

Some traditional K_D values of approximately $10^{3.70}$ have been reported for Np(V)-carbonate interactions (Ames and Rai, 1978; Harvey, 1981).

3.4 Plutonium (Pu)

Higgo and Rees (1986) studied plutonium sorption from sea water by a natural carbonate sediment. No attempt was made to control plutonium oxidation states. An initial Pu concentration of $10^{-9.64}$ M was reacted with a wide range of solid/solution ratios. The sorption behavior of plutonium was found to be complex. At solid/solution ratios greater than 40 g/l, K_D values ranging from $10^{2.0}$ to $10^{2.3}$ were obtained, and the Pu was present in oxidized states. Lower solid/solution ratios yielded K_D values greater than $10^{4.0}$ and the Pu was present in reduced forms. The low K_D values obtained at high solid/solution ratios were accounted for by the formation of Pu-carbonate solution complexes that sorb less effectively.

Gromov and Spitsyn (1974) investigated the adsorption of plutonium by heterogeneous carbonate bottom sediments in sea water. Sediment surface area was taken into account, temperature ranged from 22-24°C, and the solid/solution ratio varied from 0.1 to 1.2 g/l. Preconditioned flasks were stirred vigorously with Pu-spiked sea water and sediment until solution steady state was attained in approximately one hour. The amount of sorption was determined by the change in radioactivity of the solution phase. Sorption isotherms indicated that Pu had at least one sorbable form, likely a $Pu(OH)_m^{n+}$. At higher solid/solution ratios the presence of unsorbable forms became apparent, probably due to complexation with carbonate or organic matter. The K_D reported for plutonium with the carbonate sediment was $10^{4.04}$.

Ginzburg and Maksimov (1975) investigated the coprecipitation of Pu(IV) with calcium carbonate. Initial plutonium concentrations varied from 10^{-5} to 10^{-9} M. Steady-state conditions occurred within 30 minutes after the initiation of precipitation. Pu(IV) entrainment was greatest when a large amount of calcite precipitated. If Pu^{4+} was introduced into solution after the initiation of calcite precipitation, a much lower percentage of removal occurred. An increase in carbonate ion concentration decreased Pu^{4+} entrainment by the precipitate in all cases. This decrease could have been due to carbonate complexation in solution, or an artifact of the precipitate crystal form. At high carbonate alkalinities, small spherical aggregates with radial structure formed; lower carbonate alkalinities produced larger rhombohedral crystals. The spherical aggregates were more susceptive to surface sorption, whereas the prismatic crystals incorporated more Pu^{4+} into the bulk of the crystal.

Dosch (1979) studied plutonium sorption onto dolomite and reported K_D values of $10^{3.86}$ from AGW and $10^{3.32}$ from a halite brine. Dosch and Lynch (1980) found similar values for Pu sorption onto natural dolomite and protodolomites; their K_D values ranged from $10^{3.30}$ to $10^{3.85}$.

3.5 Radium (Ra)

Gnanapragasam (1991) studied the partitioning of radium between calcium carbonate and solutions slightly supersaturated with respect to calcite, over reaction periods of 8 and 17 weeks. Seeded experiments yielded slightly higher partition coefficients compared to homogeneous nucleation. A logarithmic partition coefficient of $\lambda = 10^{-1.89}$ was found to be valid for the range $[Ra^{2+}]_{aq}:[Ca^{2+}]_{aq} = 10^{-9}$ to 10^{-6} or $[Ra]_{solid}:[Ca]_{solid} = 10^{-10}$ to 10^{-8}. Below an aqueous $Ra^{2+}:Ca^{2+}$ ratio of 10^{-9}, λ increased to an unspecified value.

3.6 Thorium (Th)

Carroll et al. (1992) captured BEI images of a thorium-reacted calcite crystal which exhibited thorium-rich regions along rhombohedral cleavage faces. The images provided direct evidence that thorium forms a solid solution with calcite.

Stout and Carroll (in progress) are conducting a rigorous thermodynamic and kinetic study of the Th(IV)-calcite system.

3.7 Uranium (U)

Carroll and Bruno (1991) investigated U(VI)-calcite interactions within a thermodynamic and kinetic framework. The overall capacity for calcite to remove U(VI) from solution was very small and limited to monolayer coverage in solutions undersaturated with respect to rutherfordite, $UO_2CO_3(s)$. Less than 2% of the initial UO_2^{2+} was removed from solution. The limited incorporation of UO_2^{2+} at near-neutral pH was a result of the formation of uranyl-carbonato complexes and the structure of the UO_2^{2+} complex; the linear structure of the complex is too large to fit into the calcite lattice.

The kinetics of UO_2^{2+}-calcite interactions were studied with a thin-film continuous-flow reactor. This device allowed investigation of the interactions as a function of solution composition without disturbing the solid phase, and it simulated the movement of ground water past the mineral phase. Initial UO_2^{2+} concentrations varied from $10^{-4.5}$ to 10^{-2} M. A $CO_2(g)$ pressure of 0.97 atmospheres and a $10^{-2.30}$ M $NaHCO_3$ background electrolyte solution were used. The solid phase was reacted with increasingly concentrated input solutions. Filtered samples were taken periodically for analysis over a 40-hour period.

Interactions in the U(VI)-calcite system may be described as the adsorption of U(VI) at the calcite solution interface:

$$UO_2^{2+} + CaCO_3(s) \leftrightarrow >UO_2CO_3 + Ca^{2+} \tag{34}$$

and the corresponding mass balance expression:

$$K_{ex}^{*} = \frac{\{Ca^{2+}\}[>UO_2CO_3]}{\{UO_2^{2+}\}\{CaCO_3(s)\}} \tag{35}$$

where $[>UO_2CO_3]$ is equal to the mole fraction of U(VI) at the calcite surface. K_{ex}^{*} equaled $10^{-5.12\pm0.53}$ and was independent of solution pH.

In a related study, Carroll et al. (1992) investigated the interaction of U(VI) with the calcite-solution interface by using SEM, BEI, and Rutherford backscattering spectroscopy (RBS). Experimental work was conducted at 50°C and $CO_2(g)$ pressures of 0.97 and 0.1 atm. Cleaved

crystal fragments and powdered calcite were exposed to initial U(VI) concentrations below $10^{-2.64}$ M in a $10^{-2.30}$ M $NaHCO_3$ background solution.

Precipitation of a uranium bearing phase occurred only in those solutions supersaturated with respect to rutherfordite, $UO_2CO_3(s)$. At a UO_2^{2+} concentration of $10^{-3.66}$ M and pH 8, two different growth morphologies existed: flat, radial growths containing U- and Ca-rich bands, and small calcite rhombs. The radial growths presumably began as uranium carbonate nucleated on the surface, and the zoning possibly reflected changes in solution composition during reaction time. At pH 4.3, nearly parallel anastamosing uranium-bearing growths occurred within the calcite surface. RBS analysis of the pH 4.3 sample revealed minimal solid solution at depth, supporting the conclusions of Carroll and Bruno (1991).

Morse et al. (1984) attempted to establish the relation between uranyl speciation and sorption behavior with synthetic calcite and aragonite, two biogenic carbonates, and a carbonate sand (50/50 mix of biogenic aragonite and Mg-calcite). The primary goals of the study were to establish the influences of the mineral phase, solid/solution ratio, solution composition, and initial UO_2^{2+} concentration on sorption.

Initial experiments investigating the extent of uranyl adsorption onto calcite yielded unusual results. UO_2^{2+} adsorbed rapidly and then slowly desorbed back into solution. Simultaneously, a series of solution color changes occurred, indicating changes in UO_2^{2+} complexation behavior. Changing the solid/solution ratio had a minor effect on the extent of adsorption, though the reaction kinetics were approximately proportional to the solid/solution ratio. The extent and kinetics of UO_2^{2+} adsorption on calcite were similar in all solutions, varying by approximately 10%. Biogenic carbonates adsorbed UO_2^{2+} slowly, reflecting their lower effective surface areas. The most significant influence on UO_2^{2+} adsorption was the initial concentration. At initial UO_2^{2+} concentrations below approximately 10^{-5} M, little adsorption occurred. With increased UO_2^{2+} concentration, the extent of adsorption increased to nearly 100%, until at uranyl concentrations greater than 10^{-2} M, maximum adsorption decreased to less than 20%.

Morse et al. (1984) noted that significant adsorption did not occur until the UO_2^{2+} concentration approached the carbonate alkalinity. This result suggested that adsorption is related to the availability of bicarbonate and carbonate anions in solution for complex formation. The authors suggest that UO_2^{2+} adsorbed initially through the formation of hydroxy-carbonato surface species,

and when an equilibrium concentration of HCO_3^-/CO_3^{2-} was established, the UO_2^{2+} surface complex was removed from the calcite-solution interface by the formation of uranyl-carbonato complexes.

Milton and Brown (1987) examined uranyl sorption by a variety of minerals, including calcite. Synthetic and natural calcite chips were exposed to low ionic strength, pH 8.5 ground water. Initial uranyl concentrations were well below the solubility limit of rutherfordite, $UO_2CO_3(s)$. Approximately 90% of the added UO_2^{2+} was quickly adsorbed. Over extended reaction periods, a portion of the initially adsorbed UO_2^{2+} desorbed, eventually reaching a steady state at approximately 70% adsorption. When desorption was induced by solution replacement, roughly 10% of the adsorbed UO_2^{2+} desorbed after one day. Desorption continued slowly and no steady state was attained within 145 days. The authors suggest that adsorbed UO_2^{2+} ions were incorporated into the calcite lattice as a solid solution, and the later dissolution of the solid solution controlled the long-term aqueous uranyl concentration.

Kitano and Oomori (1971) investigated the coprecipitation of uranium with various calcium carbonate phases. Uranyl-bearing Mg-poor calcite, Mg-rich calcite, and aragonite were selectively precipitated from calcium bicarbonate solutions by decarboxylation. Controlling the amount of $MgCl_2$ or Na-citrate present in solution determined which carbonate phase precipitated. At measured time intervals, aliquots of the supernatant were withdrawn to determine changes in pH, Ca^{2+} concentration, and UO_2^{2+} concentration with time. At the end of each experiment, the solid was split into two portions. The first portion was analyzed for chemical composition, and the second portion was analyzed by powder x-ray diffraction (XRD) to identify crystallinity.

Kitano and Oomori (1971) described calcium-uranyl-carbonate coprecipitation with the logarithmic partition coefficient, Equation 3. For the uranyl-calcite coprecipitate, $\lambda_{calcite}$ ranged from $10^{-2.0}$ to $10^{-0.7}$. The value of $\lambda_{aragonite}$ was generally an order of magnitude higher, ranging from $10^{-0.52}$ to 10^{-0}. The partition coefficients for calcite and aragonite both decreased with increasing calcium carbonate precipitation. Kitano and Oomori explain this trend as an increase in carbonate complexation in solution. As carbonate precipitation increased, pH and alkalinity also increased and reduced the activity of UO_2^{2+}; thus, the partition coefficient decreased. Because $UO_2CO_3(s)$ is orthorhombic like aragonite, the coprecipitation of uranyl with aragonite was considered in a state of equilibrium, but coprecipitation with calcite was not. The authors speculate that the large UO_2^{2+} cation fit better into the larger aragonite structure, and this accounted for the higher partition coefficients for aragonite.

The authors explored the thermodynamics of the aragonite-$MgCl_2$-NaCl-UO_2^{2+} system in some detail. For the exchange reaction:

$$UO_2^{2+} + CaCO_3(s) \leftrightarrow UO_2CO_3(s) + Ca^{2+} \tag{36}$$

the thermodynamic exchange constant between aragonite and uranyl ions is:

$$K_{ex} = \frac{\{Ca^{2+}\}\{UO_2CO_3(s)\}}{\{UO_2^{2+}\}\{CaCO_3(s)\}} = \frac{K_{sp}(\text{aragonite})}{K_{sp}(UO_2CO_3)} = \frac{10^{-8.22}}{10^{-11.73}} = 10^{3.48} \tag{37}$$

Once uranyl-carbonate complexation was accounted for in the partition coefficient, complete agreement was found between the experimental λ and K_{ex} values for the aragonite system without NaCl. Significant unexplained differences existed for the same system with NaCl.

4.0 TRACE METALS

Very few controlled thermodynamic or kinetic studies in the actinide-carbonate system were found in the survey of published literature. Therefore, a few studies pertaining to other metal-carbonate systems are discussed here. These studies present the most promising approaches and methods in the literature today. Table 4-1 summarizes the reviewed trace metal-carbonate studies. An additional reference list of trace element-carbonate studies is provided in the appendix.

Table 4-1. Summary of Reviewed Trace Metal-Carbonate Mineral Research

Author	Sorbate	Sorbent	Background solution	Experiment type	Value	Comments
Zachara et al. (1991)	Ba^{2+}, Sr^{2+} Cd^{2+} Mn^{2+} Co^{2+} Ni^{2+} Zn^{2+}	calcite	DI	exchange	n/a $K^*_{ex} = 10^{3.02}$ $K^*_{ex} = 10^{1.31}$ $K^*_{ex} = 10^{0.56}$ $K^*_{ex} = 10^{0.51}$ $K^*_{ex} = 10^{1.50}$ to $10^{3.00}$	n/a
Comans and Middelburg (1987)	Cd, Mn Zn, Co	calcite	various	surface precipita-tion	n/a	n/a
Davis et al. (1987)	Cd(II)	calcite	AGW 0.1M NaCl-$MgCl_2$	exchange kinetic partition	$D = 10^{3.18}$ $K_{ex} = 10^{2.83}$	D experimental K_{ex} calculated
Papadopoulos and Rowell (1988)	Cd(II)	calcite	DI	partition (surface)	$D^* = 10^{3.50}$ $K_{ex} = 10^{3.52}$	D experimental K_{ex} calculated
Stipp et al. (1992)	Cd(II)	calcite	DI	surface	n/a	XPS, LEED, AES
Zachara et al. (1988)	Zn(II)	calcite	DI	exchange	$K^*_{ex} = 10^{1.00}$ to $10^{2.17}$ $K_{ex} = 10^{3.52}$	experimental calculated
Jurinak and Bauer (1956)	Zn	calcite dolomite Ca-magnesite	0.01 NaCl	isotherm	n/a	n/a
Zachara et al. (1989)	Zn	calcite	DI	surface	n/a	SEM, XPS, XRD, EDS

4.1 Comparative Studies

Zachara et al. (1991) investigated the sorption of Ba^{2+}, Sr^{2+}, Cd^{2+}, Mn^{2+}, Zn^{2+}, Co^{2+}, and Ni^{2+} onto calcite. Variations in metal properties (such as ionic radius, hydration energy, and end-

member solubility) influence cation affinity for calcite surfaces and determine the relative contributions of adsorption and precipitation.

Metal cation sorption onto calcite surfaces may be expressed by a surface exchange reaction:

$$>Ca + Me^{2+} \leftrightarrow >Me + Ca^{2+} \quad (38)$$

and the surface exchange constant, K^*_{ex}, is equal to:

$$K^*_{ex} = \frac{[Ca^{2+}]}{[Me^{2+}]} \left\{\frac{X^*_{Me}}{X^*_{Ca}}\right\}^n \quad (39)$$

where X*, the surface mole fraction, equals the amount of sorbed Me divided by S_T, and n is an empirical constant. When n = 1, the sorption isotherms have unit slope, and a single exchange constant may describe the sorption reaction.

Initial trace metal concentrations varied from 10^{-8} to 10^{-4} M. The adsorbate was an aged synthetic calcite of known surface area. Samples of the same calcite were used for each sorption experiment. Solution pH ranged from 7.0 to 9.5 at atmospheric pressure of $CO_2(g)$. A series of $^{45}Ca^{2+}$ isotopic exchange experiments conducted from pH 8.4 to 9.0 yielded an average surface-site concentration of $10^{-5.44}$ mol Ca/g.

In solutions undersaturated with respect to pure metal carbonates, significant adsorption of all metals except Sr^{2+} and Ba^{2+} was observed. Metal ion sorption increased with increasing pH and decreasing aqueous Ca^{2+} maintained by calcite solubility. The sequence of observed sorption preference was Cd > Zn ≥ Mn > Co > Ni > Ba ≈ Sr. Metals with ionic radii greater than Ca^{2+} (Ba^{2+}, Sr^{2+}) sorbed weakly, whereas metals with ionic radii smaller than Ca^{2+} (Cd^{2+}, Mn^{2+}, Zn^{2+}, Co^{2+}, Ni^{2+}) sorbed strongly and exhibited metal-specific selectivity for the calcite surface. For cations smaller than Ca^{2+}, the extent of adsorption decreased with decreasing ionic radius. Desorption preference correlated well with cation hydration energy. Strongly hydrated cations (such as Zn^{2+}, Co^{2+}, and Ni^{2+}) exhibited 80% desorption within 8 hours. Cations of lower hydration energy (Cd^{2+} and Mn^{2+}) exhibited only 10 to 25% desorption.

The sorbates Cd^{2+}, Mn^{2+}, Co^{2+}, and Ni^{2+} exhibited ideal exchange behavior (n = 1) and K^*_{ex} was calculated to be $10^{3.02}$, $10^{1.31}$, $10^{0.56}$, and $10^{0.51}$, respectively. Zn^{2+} behavior differed from the other sorbates (n = 1.86) and required exchange constants that varied from $10^{1.5}$ to $10^{3.0}$, implying that calcite surface sites exhibited heterogeneity in their binding energy with Zn^{2+}. Values of K^*_{ex} were found to correlate well with ionic radius. The value for K^*_{ex} decreased as Me^{2+} radii deviated from the Ca^{2+} radius. K^*_{ex} was also found to be directly proportional to pure end-

member solubility products, which were similar in trend and magnitude to homogeneous partition coefficients reported by other researchers.

Comans and Middelburg (1987) investigated the sorption of Cd^{2+}, Mn^{2+}, Zn^{2+}, and Co^{2+} on calcite and tested the applicability of the surface precipitation model derived by Farley et al. (1985) for metal oxides. Previous research provided the data for isotherm construction (Jurinak and Bauer, 1956; Kornicker et al., 1985; McBride, 1979; McBride, 1980). Experimental conditions and data reporting varied by author, causing some problems, but with minor assumptions the data fit the model well.

The basis of the surface precipitation model is that adsorbing cations effectively become part of the adsorbent, creating new surface reaction sites for urther adsorption. Adsorption can then occur onto the new sites, incorporating the previously adsorbed cation into the solid. The continuum between adsorption and precipitation may be mathematically modeled as a "BET-like" sorption isotherm for a constant pH. Such an isotherm consists of three parts. At low Me concentrations, surface coverage increases rapidly up to monolayer coverage. With further Me addition, surface coverage remains fairly constant until the onset of precipitation, when surface coverage again increases rapidly as shown in Figure 2-1.

The equation that defines surface coverage, Γ_{Me} (total moles of Me^{2+} sorbed per mole of total moles Ca) is:

$$\Gamma_{Me} = \frac{[>MeCO_3]+[MeCO_3(s)]}{Ca_T} \tag{40}$$

This equation was expanded by the use of the pure end-member solubility products, K_{sp}, the adsorption constant, K_{ads} (see Equation 18), and applicable mass-balance equations (see Equations 20 to 22). The expanded form allowed the construction of sorption isotherms which provided a good fit to the experimental data. The apparent adsorption affinity $Cd^{2+} > Mn^{2+} > Zn^{2+} > Co^{2+}$ was as expected from the comparison of trace metal ionic radii to Ca^{2+}.

4.2 Single Element Studies

4.2.1 Cadmium: Studies of the Aqueous Phase

Davis et al. (1987) described Cd^{2+} sorption and solid solution formation at calcite surfaces based on observation and analysis of solution compositions. A solid solution consisting of $CdCO_3(s)$ and $CaCO_3(s)$ may be described by the exchange of cations between the solid and solution:

$$Cd^{2+} + CaCO_3(s) \leftrightarrow CdCO_3(s) + Ca^{2+} \tag{41}$$

and the corresponding mass-action expression:

$$K_{ex} = \frac{\{CdCO_3(s)\}\{Ca^{2+}\}}{\{CaCO_3(s)\}\{Cd^{2+}\}} \tag{42}$$

which reduces to the solubility-products ratio of the end-member carbonates:

$$K_{ex} = \frac{K_{sp}(CaCO_3(s))}{K_{sp}(CdCO_3(s))} \tag{43}$$

From the experimentally determined mole fractions of each component, the homogeneous partition coefficient for the solid solution may be determined:

$$D = \frac{\{Ca^{2+}\}X_{CdCO_3}}{\{Cd^{2+}\}X_{CaCO_3}} \tag{44}$$

The mole fractions of the pure phases in the solid solution are related to the activities of the component solids by:

$$\gamma_{CdCO_3} X_{CdCO_3} = \{CdCO_3(s)\} \tag{45}$$

$$\gamma_{CaCO_3} X_{CaCO_3} = \{CaCO_3(s)\} \tag{46}$$

If $\gamma_{Ca^{2+}} = \gamma_{Cd^{2+}}$ and the mole fraction of $CdCO_3(s)$ is very small, such that $\gamma_{CaCO_3(s)}$ approaches unity, then:

$$\gamma_{CdCO_3(s)} D = K_{ex} \tag{47}$$

Therefore, the values of K_{ex} and D will be equal if the solid solution is ideal.

Two synthetic calcites of known purity and surface area were used in the adsorption experiments of Davis et al. (1987). Solution phases were (1) a low ionic strength AGW, and (2) synthetic solutions of 0.1 M ionic strength with varied concentrations of $MgCl_2$ and NaCl.

The solutions were equilibrated with calcite at seven different $CO_2(g)$ pressures. Initial dissolved Cd^{2+} concentrations ranged from 10^{-7} to 10^{-6} M and solid/solution ratios were varied with each experiment. Cd^{2+} activity was controlled by a slight excess of EDTA (ethylene-diaminetetraacetic acid), which, when used in trace quantities, buffered the Cd^{2+} concentration but had a negligible effect on the activity of Ca^{2+} or other major cations.

Cd^{2+} uptake from EDTA-buffered AGW indicated that at least two sorption processes occurred. Step I consisted of an initial rapid reaction that reached completion within 24 hours. Step II was a slow process that did not reach equilibrium within eight days. Step I may be further divided into two parts: step IA refers to the rapid initial uptake, likely due to adsorption of Cd^{2+} to discrete sites on the calcite surface; step IB represents the diffusion of Cd^{2+} into a hydrated $CaCO_3(s)$ layer and progressively slower sorption leading into step II.

The pH dependence of Cd^{2+} sorption upon calcite was determined from pH 6 to 8. Sorption of Cd^{2+} decreased substantially with increasing pH over a constant time interval. The decrease in Cd^{2+} adsorption with increasing pH is unusual; Davis et al. (1987) explain it by considering the pH dependence of Cd^{2+} speciation with EDTA. Addition of Mg^{2+} at constant pH and 0.1 M ionic strength caused decreases in both the magnitude of Cd^{2+} sorption in step I and the rate of uptake in step II.

Reversibility experiments used two methods: isotopic exchange of ^{109}Cd, and EDTA additions. Isotopic exchange experiments consisted of partial replacement of the supernatant with an equivalent volume and strength Cd^{2+} radiotracer spiked solution. After a short reaction time (longer reaction times did not alter results) the change in radiotracer activity enabled calculation of the rapidly exchangeable fraction of sorbed Cd^{2+}. Much of the Cd^{2+} sorbed during step I could undergo rapid exchange. However, the isotope-exchange ability of Cd^{2+} decreased significantly after increased sorption time. This decrease suggested that Cd^{2+} forms rapidly reversible bonds with surface sites at the beginning of step I, and subsequent surface reactions or mass transport into the calcite remove the Cd^{2+} from this rapidly reversible state.

The release of sorbed Cd^{2+} after addition of EDTA was compared to the results of studies where EDTA was added at the beginning of the experiment. After EDTA addition to previously unbuffered solutions, partial desorption occurred during the first four hours. The extent of Cd^{2+} desorption decreased significantly in samples that had aged longer without EDTA. Thus, with increased time before EDTA addition, Cd^{2+} became less available for release into the aqueous phase.

The variation in sorption rates between steps I and II suggested that two or more sorption processes were responsible for the removal of Cd^{2+} from solution. The rate of Cd^{2+} sorption in step I was solid-diffusion limited, and it appeared to reach completion within 24 hours. After this period, less than 10% of adsorbed Cd^{2+} would undergo isotopic exchange, suggesting that much of the Cd^{2+} had diffused into the solid (or a hydrated surface layer) and exchanged for Ca^{2+}.

A combination of Cd^{2+} sorption and Ca^{2+} isotopic exchange data supported the development of a solid solution by an exchange reaction in step II. In a previous experiment, the authors concluded that long-term Ca^{2+} isotopic exchange (equivalent to step II) was a result of recrystallization. In the presence of Cd^{2+}, recrystallized matter grows as a solid solution rather than as pure calcite. The mole fractions of $CdCO_3$ and $CaCO_3$ in the new crystalline material may be equated with the ratio of the rates of Cd^{2+} sorption in step II and long-term Ca^{2+} isotopic exchange. This ratio allows calculation of the homogeneous partition coefficient for the new crystalline material. An average value of $D = 10^{3.18 \pm 0.10}$ was found. The difference between this experimental value and the theoretical K_{ex} of $10^{2.83}$ suggested that the solid solution was not ideal and the activity coefficient of the $CdCO_3$ component was less than unity.

Papadopoulos and Rowell (1988) also investigated Cd(II)-calcite interactions. The initial reaction between Cd^{2+} and $CaCO_3(s)$ surfaces was rapid, especially at low Cd^{2+} concentrations. In more concentrated solutions close to $CdCO_3(s)$ saturation, a slow process occurred after the initial rapid sorption. The slow process was interpreted as either the precipitation of $CdCO_3$ (slow at low degrees of supersaturation) or the coprecipitation of $CdCO_3(s)$ and $CaCO_3(s)$ during recrystallization.

The homogeneous partition coefficient for the $CaCO_3$-$CdCO_3$ solid solution can be calculated from the expression:

$$D = \frac{\{Ca^{2+}\}X_{CdCO_3}}{\{Cd^{2+}\}X_{CaCO_3}} \tag{48}$$

Experimental values of D were very small, indicating an exclusion of Cd^{2+} from the bulk solid. If a two-dimensional solid solution existed and only the surface Ca^{2+} atoms were considered, then $X^*_{CdCO_3}$ and $X^*_{CaCO_3}$ represent the surface mole fractions. Using these assumptions at Cd^{2+} concentrations below $CdCO_3(s)$ saturation, a surface partition coefficient, D*, with a mean value

of $10^{3.50}$ was calculated. This value compared well with K_{ex} calculated from the ratio of the solubility products:

$$K_{ex} = \frac{K_{sp}(CaCO_3)}{K_{sp}(CdCO_3)} = \frac{10^{-8.48}}{10^{-12.0}} = 10^{3.52} \quad (49)$$

The similarity of D* and K_{ex} indicated that the solid solution was nearly ideal at the calcite surface.

4.2.2 Cadmium: Study of the Solid Phase

Stipp et al. (1992) examined the uptake of Cd^{2+} by calcite and its subsequent solid-state diffusion into the calcite lattice. The authors made extensive use of surface analysis techniques (x-ray photoelectron spectroscopy [XPS], low energy electron diffraction [LEED], and Auger electron spectroscopy [AES]). In the past, solid-state diffusion was considered unimportant in trace metal uptake from solution. The authors have shown that Cd^{2+} diffuses into the bulk of the calcite crystal and Ca^{2+} diffuses outward to form a solid solution.

Cleaved calcite crystal fragments and aged otavite ($CdCO_3$) or calcite powders were used in the adsorption and precipitation experiments. Single calcite crystals exposed to Cd^{2+} solutions were swept dry with a stream of high purity N_2 gas to avoid evaporation that could leave a residual layer on the surface. Solution compositions were chosen to specifically elicit either adsorption or precipitation. In the first portion of the study, otavite overlayers were precipitated onto calcite chips from a slightly supersaturated cadmium carbonate solution. The precipitated coating was almost pure otavite to a depth of 30 Å, as determined by XPS. The Cd:Ca ratio increased from zero on the original calcite to about 65 after two months of reaction. In contrast, the Cd:Ca ratio on calcite cleavage fragments exposed for 10 months was approximately 3:0, suggesting that over long time periods cadmium moved away from the surface. In the next experiment, a calcite chip with a surface Cd:Ca ratio of approximately 65 was stored in a vacuum for one month. During storage the surface Cd:Ca ratio decreased to a much lower value. These two experiments supported the hypothesis of solid solution development by solid-state diffusion.

The adsorption of Cd^{2+} by calcite powder was examined in solutions containing $10^{-6.4}$ M Cd^{2+}, 10^{-2} M KOH, and pure $CO_2(g)$. Seventy-five percent of the Cd^{2+} was removed from solution after 55 hours, yielding a calculated surface coverage of about one-quarter of a monolayer. If all the cadmium was present at the surface, XPS signals should have shown distinctive cadmium peaks, but none were detected. However, a widening of the calcite peaks indicated that more than

one structural environment existed in the calcite lattice, which was interpreted as resulting from Cd^{2+} substitution in the calcite lattice.

Three calcite chips were exposed to a 10^{-4} M Cd^{2+} solution spiked with a $^{109}Cd^{2+}$ radiotracer at atmospheric $CO_2(g)$ pressure for 1, 10, and 100 minutes. Scintillation counting of both the solution and the chips indicated an uptake of 1.0, 2.8, and 4.0 monolayers, respectively. One to two days later, surface analyses showed cadmium peaks for all three samples barely above background. Samples with originally higher Cd^{2+} uptake, when analyzed after longer storage times, had lower cadmium peak intensity ratios. This result, combined with the results from the calcite powder experiment, provided additional evidence for diffusion of Cd^{2+} into the bulk calcite crystal.

Stimulated desorption by x-ray exposure was used to gain useful information. Four cleavage fragments were exposed for one minute to a 10^{-4} M Cd^{2+} solution spiked with a Cd-radiotracer. Surface uptake was calculated to be about one monolayer. Two samples were analyzed within an hour of drying, and the other two samples were stored for 24 hours before analysis. The fresher samples lost 30% of their total cadmium by x-ray induced desorption, while samples stored for one day lost only around 12%. This difference demonstrated that the amount of cadmium available for x-ray stimulated desorption decreased substantially with time after uptake because the cadmium had moved away from the surface, providing further evidence for cadmium diffusion into the calcite crystal.

4.2.3 Zinc: Studies of the Aqueous Phase

Zachara et al. (1988) investigated the surface reaction mechanisms of Zn^{2+} on calcite. Zinc adsorption, desorption, and isotopic exchange were consistent with a reversible surface exchange reaction:

$$>Ca^{2+} + Zn^{2+} \leftrightarrow >Zn^{2+} + Ca^{2+} \qquad (50)$$

and the corresponding surface exchange reaction constant, K^{*}_{ex}:

$$K^{*}_{ex} = \frac{\{Ca^{2+}\}}{\{Zn^{2+}\}} \left[\frac{X^{*}_{Zn}}{X^{*}_{Ca}}\right]^{n} \qquad (51)$$

where X*, the surface mole fraction, equals the amount of sorbed Me divided by S_T, and n is an empirical constant. On a plot of $\log(\{Zn^{2+}\}/\{Ca^{2+}\})$ versus $\log(X_{Zn}/X_{Ca})$, n (the slope of the

line) equaled 1.69. The charge and speciation of the surface species (>Ca or >Zn) is unknown. This study viewed adsorption as a free cation bound to an anionic site within the lattice of a surface layer.

Experiments were conducted over various reaction times, pH values, $CO_2(g)$ pressures, Ca^{2+} concentrations, and calcite surface charges. Synthetic $CaCO_3(s)$ of known surface area and over 99% purity was the substrate for the adsorption experiments. Equilibrium calcite suspensions ranged over 2.5 pH units at three different $CO_2(g)$ pressures and a constant ionic strength of 0.1 M. Initial Zn^{2+} concentrations ranged from 10^{-7} to 10^{-4} M.

Sorption studies were conducted under conditions undersaturated with respect to the most stable phase, hydrozincite, $Zn_5(OH)_6(CO_3)_2(s)$. Initial removal of Zn^{2+} from solution was rapid. After approximately 12 hours, sorption either ceased entirely or continued with first order reaction kinetics. The amount of zinc adsorbed was a function of the initial Zn^{2+} concentration, the substrate surface area, and the calcite used. Sorption increased with increased pH; simultaneously Ca^{2+} concentrations decreased and carbonate alkalinity increased due to calcite solubility. At any single initial Zn^{2+} concentration, fractional adsorption increased with increased pH, yielding a pH-edge similar to that of metal oxide adsorption. The majority of linear and log-log sorption isotherms displayed a reduction in slope at a surface density of $10^{-6.5}$ to $10^{-6.3}$ moles-Zn/m^2, which represents an empirical measure of the adsorption maximum.

The extent of desorption depended upon the methodology of solution change. Replacing the electrolyte solution while maintaining the pH and Ca^{2+} concentrations caused very limited desorption. Drastic lowering of pH levels caused complete reversibility by altering the equilibrium of the calcite suspension. K_{ex}, expressed as the ratio of the solubility products of pure end-member solid phases, is equal to:

$$K_{ex} = \frac{K_{sp}(CaCO_3)}{K_{sp}(MeCO_3)} = 10^{2.32} \tag{52}$$

This value defines a thermodynamic equilibrium constant for solid solution formation or distribution in a solid phase. When a surface-site density of $10^{-5.08}$ mol-Ca/m^2 was assumed for calcite (estimated from calcite crystallography) and combined with the adsorption data, the experimental value of K^*_{ex} was found to be

$$K^*_{ex} = \frac{\{Ca^{2+}\}X^*_{Zn}}{\{Zn^{2+}\}X^*_{Ca}} \approx 10^{1.0} \text{ to } 10^{2.17} \tag{53}$$

Because this value was lower than the predicted thermodynamic value, the authors speculated that solubility product ratios may not be good predictors of sorption when surface exchange, rather than coprecipitation, is the mechanism.

Jurinak and Bauer (1956) examined zinc adsorption on calcite, dolomite, and 5.8 mol-% Ca-magnesite. Zinc adsorption on calcite decreased with increased temperature, indicating an exothermic reaction. A plateau on the sorption isotherms indicated a region of surface saturation followed by increased adsorption at a Zn^{2+} concentration of approximately $10^{-5.37}$ M. Because multilayer adsorption of cations is rare, the authors hypothesized that the increased adsorption must be due to a second type of adsorption site.

Zn^{2+} adsorption on dolomite exhibited no isotherm plateaus indicating site saturation. Additionally, increased temperature caused an increase rather than a decrease in adsorption, indicating an endothermic reaction. Adsorption of Zn^{2+} by Ca-magnesite was also endothermic, and showed the highest extent of Zn^{2+} adsorption. Increasing the Mg content of the sorbent increased the maximum extent of Zn^{2+} adsorption. The source of adsorptive differences introduced by an increased Mg:Ca ratio of the sorbent may have been due to the differing interionic distances in the crystal lattice. It is worth noting that the ionic radii of Mg^{2+} and Zn^{2+} are very similar (0.78 and 0.83 Å, respectively) which suggests the possibility of an exchange reaction.

4.2.4 Zinc: Study of the Solid Phase

Zachara et al. (1989) examined the solubility and surface spectroscopy of zinc precipitates on calcite. The precipitation of zinc phases from equilibrium calcite suspensions was investigated to determine if the calcite surface would assist nucleation of zinc solid phases. The presence of calcite was not a requisite for precipitation, though the precipitate was associated with the calcite surface when present. The surface analysis techniques SEM, XPS, XRD, and EDS were used to characterize the surface precipitates. After contact with 10^{-5} and 10^{-4} M Zn^{2+} solutions calculated to be supersaturated with respect to hydrozincite, no visual or spectroscopic evidence of zinc precipitates was found on the calcite surface. The precipitate was either too small to be resolved or was a very thin coating: even at 20,000-x magnification no visible evidence of precipitation existed.

Small, plate-like flecks nucleated on the calcite surface after exposure to 10^{-3} M Zn^{2+} solutions. EDS analysis confirmed the presence of zinc in the precipitate, and subsequent XRD

analysis yielded a pattern very similar to hydrozincite. The of Zn-precipitate was less soluble than natural smithsonite, $ZnCO_3(s)$, and more soluble than natural hydrozincite; the difference was ascribed to unquantifiable structural and hydration differences. The precipitation of hydrozincite appeared to be kinetically favored over smithsonite, which is thermodynamically more stable and isostructural with calcite.

5.0 CONCLUSION

It is apparent from this review that research into actinide-carbonate interactions is embryonic at best. The majority of accessible data is in the form of phenomenological distribution or partition coefficients. Many problems exist in past and present-day experimental design. The use of brines, sea water, etc. is useful for descriptive purposes and application to site-specific storage problems, but it complicates the fundamental understanding of the processes at work by introducing additional variables into an already complex situation. Furthermore, radionuclide solubility, speciation, complexation, and redox response all need to be addressed and integrated into existing geochemical computer codes. Research into the interface geochemistry of Am, Nd, Pu, and U, while incomplete, at least is supported by considerable data. Studies of the behavior of Cm, Ra, and Th in the geosphere are virtually nonexistent.

The success of geochemical modeling lies in the integration of thermodynamic, kinetic, and surface studies. Exchange models provide a firm theoretical basis, and could easily become a standard for research in coming years. The applications of the surface precipitation and exchange models are the most descriptive and convenient methods for predicting aqueous metal concentrations over a broad range of conditions, providing equilibrium is obtained. The growing use of surface analysis techniques is a very promising aspect of geochemical research. The application of macroscopic techniques (e.g., solution and bulk solid composition) to atomic-scale problems simply does not suffice for a full description of interface chemistry.

6.0 REFERENCES

Allard, B. 1984. "Mechanisms for the Interaction of Am(III) and Np(V) with Geologic Media," *Scientific Basis for Nuclear Waste Management VII, Materials Research Society Symposia Proceedings, Boston, MA, November 14-17, 1983.* Ed. G.L. McVay. New York, NY: North-Holland. Vol. 26, 899-906.

Ames, L.L., and D. Rai. 1978. *Radionuclide Interactions with Soil and Rock Media.* EPA 520/6-78-007. Las Vegas, NV: US Environmental Protection Agency, Office of Radiation Programs.

Carroll, S.A. 1993. "Precipitation of Nd-Ca Carbonate Solid Solution at 25°C," *Geochimica Cosmochimica Acta.* Vol. 57, No. 14, 3383-3393.

Carroll, S.A., and J. Bruno. 1991. "Mineral-Solution Interactions in the U(VI)-CO_2-H_2O System," *Radiochimica Acta.* Vol. 52/53, pt. 1, 187-193.

Carroll, S.A., J. Bruno, J-C. Petit, and J-C. Dran. 1992. "Interactions of U(VI), Nd, and Th(IV) at the Calcite-Solution Interface," *Radiochimica Acta.* Vol. 58/59, pt. 2, 245-252.

Comans, R.N.J., and J.J. Middelburg. 1987. "Sorption of Trace Metals on Calcite: Applicability of the Surface Precipitation Model," *Geochimica et Cosmochimica Acta.* Vol. 51, no. 9, 2587-2591.

Davis, J.A., C.C. Fuller, and A.D. Cook. 1987. "A Model for Trace Metal Sorption Processes at the Calcite Surface: Adsorption of Cd^{2+} and Subsequent Solid Solution Formation," *Geochimica et Cosmochimica Acta.* Vol. 51, no. 6, 1477-1490.

Dosch, R.G. 1979. "Radionuclide Migration Studies Associated with the WIPP Site in Southern New Mexico," *Scientific Basis for Nuclear Waste Management, Proceedings of the Symposium on 'Science Underlying Radioactive Waste Management,' Boston, MA, November 28-December 1, 1978.* Ed. G.J. McCarthy. SAND78-1178. New York, NY: Plenum Press. Vol. 1, 395-398.

Dosch, R.G., and A.W. Lynch. 1980. "Radionuclide Transport in a Dolomite Aquifer," *Scientific Basis for Nuclear Waste Management, Proceedings of the International Symposium, Boston, MA, November 27-30, 1979.* Ed. C.J.M. Northrup, Jr. SAND79-1016. New York, NY: Plenum Press. Vol. 2, 617-624.

Farley, K.J., D.A. Dzombak, and F.M.M. Morel. 1985. "A Surface Precipitation Model for the Sorption of Cations on Metal Oxides," *Journal of Colloid and Interface Science.* Vol. 106, no. 1, 226-242.

Franklin, M.L., and J.W. Morse. 1982. "The Interaction of Copper with the Surface of Calcite," *Ocean Science and Engineering.* Vol. 7, no. 2, 147-174.

Ginzburg, F.L., and V.F. Maksimov. 1975. "Concentration of Plutonium(IV) and Europium by Coprecipitation with Calcium Carbonate," *Radiokhimiya.* Vol. 17, no. 1, 3-9.

Gnanapragasam, E.K. 1991. "Solubility Control of Radium by Calcium Precipitates: Experimental Determination and Theoretical Prediction of Partition Coefficients of Radium and Calcium Between the Minerals Gypsum, Brushite, or Calcite and Their Respective Solution." PhD dissertation. Evanston, IL: Northwestern University.

Gromov, V.V., and V.I. Spitsyn. 1974. "Sorption of ^{239}Pu, ^{106}Ru, and ^{99}Tc by Bottom Sediments in the Pacific Ocean," *Radiokhimiya.* Vol. 16, no. 2, 157-162.

Harvey, B.R. 1981. "Interstitial Water Studies on Irish Sea Sediments and Their Relevance to the Fate of Transuranic Nuclides in the Marine Environment," *Techniques for Identifying Transuranic Speciation in Aquatic Environments, Proceedings of a Technical Committee Meeting on the Behaviour of Transuranics in the Aquatic Environment and Sediment-Water Exchanges, Ispra, Italy, March 24-28, 1980.* Vienna, Austria: International Atomic Energy Agency. 247-256..

Higgo, J.J.W., and L.V.C. Rees. 1986. "Adsorption of Actinides by Marine Sediments: Effect of the Sediment/Seawater Ratio on the Measured Distribution Ratio," *Environmental Science and Technology.* Vol. 20, no. 5, 483-490.

Jurinak, J.J., and N. Bauer. 1956. "Thermodynamics of Zinc Adsorption on Calcite, Dolomite, and Magnesite-type Minerals," *Soil Science Society of America Proceedings.* Vol. 20, 466-471.

Keeney-Kennicutt, W.L., and J.W. Morse. 1984. "The Interaction of $Np(V)O_2^+$ with Common Mineral Surfaces in Dilute Aqueous Solutions and Seawater," *Marine Chemistry.* Vol. 15, no. 2, 133-150

Kitano, Y., and T. Oomori. 1971. "The Coprecipitation of Uranium with Calcium Carbonate," *Journal of the Oceanographic Society of Japan.* Vol. 27, no. 1, 34-42.

Kornicker, W.A., J.W. Morse, and R.N. Damasceno. 1985. "The Chemistry of CO^{2+} Interaction with Calcite and Aragonite Surfaces," *Chemical Geology.* Vol. 53, no. 3/4, 229-236.

Lorens, R.B. 1981. "Sr, Cd, Mn, and Co Distribution Coefficients in Calcite as a Function of Calcite Precipitation Rate," *Geochimica et Cosmochimica Acta.* Vol. 45, no. 4, 553-561.

McBride, M.B. 1979. "Chemisorption and Precipitation of Mn^{2+} at $CaCO_3$ Surfaces," *Soil Science Society of America Journal.* Vol. 43, no. 4, 693-698.

McBride, M.B. 1980. "Chemisorption of Cd^{2+} on Calcite Surfaces," *Soil Science Society of America Journal.* Vol. 44, no. 1, 26-28.

McIntire, W.L. 1963. "Trace Element Partition Coefficients–A Review of Theory and Applications to Geology," *Geochimica et Cosmochimica Acta.* Vol. 27, no. 12, 1209-1264.

Mecherri, O.M., P. Budiman-Sastrowardoyo, J-C. Rouchaud, and M. Fedoroff. 1990. "Study of Neodymium Sorption on Orthose and Calcite for Radionuclide Migration Modelling in Groundwater," *Radiochimica Acta.* Vol. 50, no. 3, 169-175.

Milton, G.M., and R.M. Brown. 1987. "Adsorption of Uranium from Groundwater by Common Fracture Secondary Minerals," *Canadian Journal of Earth Sciences*. Vol. 24, no. 7, 1321-1328.

Morse, J.W., P.M. Shanbhag, A. Saito, and G.R. Choppin. 1984. "Interaction of Uranyl Ions in Carbonate Media," *Chemical Geology*. Vol. 42, no. 1/4, 85-99.

Novak, C.F. 1992. *An Evaluation of Radionuclide Batch Sorption Data on Culebra Dolomite for Aqueous Compositions Relevant to the Human Intrusion Scenario for the Waste Isolation Pilot Plant*. SAND91-1299. Albuquerque, NM: Sandia National Laboratories.

Papadopoulos, P., and D.L. Rowell. 1988. "The Reactions of Cadmium with Calcium Carbonate Surfaces," *Journal of Soil Science*. Vol. 39, no. 1, 23-36.

Parks, G.A. 1990. "Surface Energy and Adsorption at Mineral Water Interfaces," *Mineral-Water Interface Geochemistry*. Eds. M.F. Hochella, Jr. and A.F. White. Reviews in Mineralogy 23. 133-176.

Pingitore, N.E., Jr. 1986. "Modes of Coprecipitation of Ba^{2+} and Sr^{2+} with Calcite," *Geochemical Processes at Mineral Surfaces, Chicago, IL, September 8-13, 1985*. Eds. J.A. Davis and K.F. Hayes. ACS Symposium Series 323. Washington, DC: American Chemical Society. 574-586.

Shanbhag, P.M., and J.W. Morse. 1982. "Americium Interaction with Calcite and Aragonite Surfaces in Seawater," *Geochimica et Cosmochimica Acta*. Vol. 46, no. 2, 241-246.

Smith, R.W. 1990. "Calculated Partitioning of Americium(III) Into Calcite: An Example of Trivalent Cation Substitution in Rhombohedral Carbonates," *Abstracts with Programs, Geological Society of America, Dallas, TX, October 29-November 1, 1990*. A261.

Stipp, S.L., M.F. Hochella, Jr., G.A. Parks, and J.O. Leckie. 1992. "Cd^{2+} Uptake by Calcite, Solid-State Diffusion, and the Formation of Solid-Solution: Interface Processes Observed with Near-Surface Sensitive Techniques (XPS, LEED, and AES)," *Geochimica et Cosmochimica Acta*. Vol. 56, no. 5, 1941-1954.

Wang, Y., and E. Merino. 1992. "Dynamic Model of Oscillatory Zoning of Trace Elements in Calcite: Double Layer, Inhibition, and Self-Organization," *Geochimica et Cosmochimica Acta*. Vol. 56, no. 2, 587-596.

Wersin, P., L. Charlet, R. Karthein, and W. Stumm. 1989. "From Adsorption to Precipitation: Sorption of Mn^{2+} on $FeCO_3(s)$," *Geochimica et Cosmochimica Acta*. Vol. 53, no. 11, 2787-2796.

Zachara, J.M., J.A. Kittrick, and J.B. Harsh. 1988. "The Mechanism of Zn^{2+} Adsorption on Calcite," *Geochimica et Cosmochimica Acta*. Vol. 52, no. 9, 2281-2291.

Zachara, J.M., J.A. Kittrick, L.S. Dake, and J.B. Harsh. 1989. "Solubility and Surface Spectroscopy of Zinc Precipitates on Calcite," *Geochimica et Cosmochimica Acta*. Vol. 53, no. 1, 9-19.

Zachara, J.M., C.E. Cowan, and C.T. Resch. 1991. "Sorption of Divalent Metals on Calcite," *Geochimica et Cosmochimica Acta.* Vol. 55, no. 6, 1549-1562.

APPENDIX A: BIBLIOGRAPHY OF ACTINIDE SPECIATION, COMPLEXATION, AND SOLUBILITY STUDIES

APPENDIX A

Bibliography of Actinide Speciation, Complexation, and Solubility Studies

Allard, B., H. Kipatsi, and J.L. Liljenzin. 1980. "Expected Species of Uranium, Neptunium and Plutonium in Neutral Aqueous Solutions," *Journal of Inorganic and Nuclear Chemistry.* Vol. 42, no. 7, 1015-1027.

Anderson, R.F., M.P. Bacon, and P.G. Brewer. 1982. "Elevated Concentrations of Actinides in Mono Lake," *Science.* Vol. 216, no. 4545, 514-516.

Brookins, D.G. 1978. "Retention of Transuranic and Actinide Elements and Bismuth at the Oklo Natural Reactor, Gabon: Application of Eh-pH Diagrams," *Chemical Geology.* Vol. 23, no. 4, 309-323.

Brookins, D.G. 1979. "Thermodynamic Considerations Underlying the Migration of Radionuclides in Geomedia: Oklo and Other Examples," *Scientific Basis for Nuclear Waste Management, Proceedings of the Symposium on 'Science Underlying Radioactive Waste Management,' Boston MA, November 28-December 1, 1978.* Ed. G.J. McCarthy. New York, NY: Plenum Press. Vol. 1, 355-366.

Bruno, J., I. Casas, I. Grenthe, and B. Lagerman. 1987. "Studies on Metal Carbonate Complexes. 19. Complex Formation in the Th(IV)-H_2O-CO_2 (g) System," *Inorganica Chimica Acta.* Vol. 140, no. 1-2, 299-301.

Bruno, J., I. Grenthe, and P. Robouch. 1989. "Studies of Metal Carbonate Equilibria. 20. Formation of Tetra(carbonato)uranium(IV) Ion, $U(CO_3)_4^{4-}$, in Hydrogen Carbonate Solutions," *Inorganica Chimica Acta.* Vol. 158, no. 2, 221-226.

Cleveland, J.M. 1979. "Critical Review of Plutonium Equilibria of Environmental Concern," *Chemical Modeling in Aqueous Systems: Speciation, Sorption, Solubility, and Kinetics, Miami Beach, FL, September 11-13, 1978.* Ed. E.A. Jenne. ACS Symposium Series 93. Washington, DC: American Chemical Society. 321-338.

Cleveland, J.M., T.F. Rees, and K.L. Nash. 1983. "Plutonium Speciation in Water from Mono Lake, California," *Science.* Vol. 222, no. 4630, 1323-1325.

Felmy, A.R., D. Rai, and R.W. Fulton. 1990. "The Solubility of $AmOHCO_3$(c) and the Aqueous Thermodynamics of the System Na^+-Am^{3+}-HCO_3^{2-}-OH^--H_2O," *Radiochimica Acta.* Vol. 50, no. 4, 193-204.

Kim, J.I., G. Buckau, F. Baumgärtner, H.C. Moon, and D. Lux. 1984. "Colloid Generation and the Actinide Migration in Gorleben Groundwaters," *Scientific Basis for Nuclear Waste Management VII, Materials Research Society Symposia Proceedings, Boston, MA, November 14-17, 1983.* Ed. G.L. McVay. New York, NY: North-Holland. Vol. 26, 31-40.

Lagerman, B. O. 1990. "*Complex Formation in the Actinoid-H_2O-$CO_{2(g)}$ System.*" PhD dissertation. Stockholm, Sweden: Royal Institute of Technology.

Langmuir, D. 1978. "Uranium Solution-Mineral Equilibria at Low Temperatures with Applications to Sedimentary Ore Deposits," *Geochimica et Cosmochimica Acta.* Vol. 42, no. 6, 547-569.

Langmuir, D., and J.S. Herman. 1980. "The Mobility of Thorium in Natural Waters at Low Temperatures," *Geochemica et Cosmochimica Acta.* Vol. 44, no. 11, 1753-1766.

Meinrath, G., and J.I. Kim. 1991a. "Solubility Products of Different Am(III) and Nd(III) Carbonates," *European Journal of Solid State and Inorganic Chemistry.* Vol. 28, 383-388.

Meinrath, G., and J.I. Kim. 1991b. "The Carbonate Complexation of the Am(III) Ion," *Radiochimica Acta.* Vol. 52/53, pt. 1, 29-34.

Nash, K.L., J.M. Cleveland, and T.F. Rees. 1988. "Speciation Patterns of Actinides in Natural Waters: A Laboratory Investigation," *Journal of Environmental Radioactivity.* Vol. 7, no. 2, 131-157.

Nelson, D.M., K.A. Orlandini, and W.R. Penrose. 1989. "Oxidation States of Plutonium in Carbonate-Rich Natural Waters," *Journal of Environmental Radioactivity.* Vol. 9, no. 3, 189-198.

Nitsche, H. 1991. "Solubility Studies of Transuranium Elements for Nuclear Waste Disposal: Principles and Overview," *Radiochimica Acta.* Vol. 52/53, pt. 1, 3-8.

Olofsson, U., M. Bengtsson, and B. Allard. 1984. "Generation and Transport of Colloidal Tri- and Tetravalent Actinide Species in Geologic Environments," *Scientific Basis for Nuclear Waste Management VII, Materials Research Society Symposia Proceedings, Boston, MA, November 14-17, 1983.* Ed. G.L. McVay. New York, NY: North-Holland. Vol. 26, 859-866.

Rai, D., R.J. Serne, and J.L. Swanson. 1980. "Solution Species of Plutonium in the Environment," *Journal of Environmental Quality.* Vol. 9, no. 3, 417-420.

Ramsay, J.D.F. 1988. "The Role of Colloids in the Release of Radionuclides from Nuclear Waste," *Radiochimica Acta.* Vol. 44/45, pt. 1, 165-170.

Sanchez A.L. 1983. "Chemical Speciation and Adsorption Behavior of Plutonium in Natural Waters (British Columbia)." PhD dissertation. Seattle, WA: University of Washington.

Silva, R.J. 1984. "The Behavior of Americium in Aqueous Carbonate Systems," *Scientific Basis for Nuclear Waste Management VII, Materials Research Society Symposia Proceedings, Boston, MA, November 14-17, 1983.* Ed. G.L. McVay. New York, NY: North-Holland. Vol. 26, 875-881.

APPENDIX B: BIBLIOGRAPHY OF TRACE METAL SORPTION/COPRECIPITATION STUDIES

APPENDIX B

Bibliography of Trace Metal Sorption/Coprecipitation

Bancroft, G.M., J.R. Brown, and W.S. Fyfe. 1977. "Quantitative X-ray Photoelectron Spectroscopy (ESCA): Studies of Ba^{2+} Sorption on Calcite," *Chemical Geology.* Vol. 19, no. 2, 131-144.

Crocket, J.H., and J.W. Winchester. 1966. "Coprecipitation of Zinc with Calcium Carbonate," *Geochimica et Cosmochimica Acta.* Vol. 30, no. 10, 1093-1109.

Davis, J.A., and K.F. Hayes. 1986. "Geochemical Processes at Mineral Surfaces: An Overview," *Geochemical Processes at Mineral Surfaces, Chicago, IL, September 8-13, 1985.* Ed. J.A. Davis and K.F. Hayes. ACS Symposium Series 323. Washington, DC: American Chemical Society. 2-18.

Franklin, M.L., and J.W. Morse. 1983. "The Interaction of Mn^{2+} with the Surface of Calcite in Dilute Solutions and Seawater," *Marine Chemistry.* Vol. 12, no. 4, 241-254.

Fuller, C.C., and J.A. Davis. 1987. "Processes and Kinetics of Cd^{2+} Sorption by a Calcareous Aquifer Sand," *Geochimica et Cosmochimica Acta.* Vol. 51, no. 6, 1491-1502.

House, W.A., and L. Donaldson. 1986. "Adsorption and Coprecipitation of Phosphate on Calcite," *Journal of Colloid and Interface Science.* Vol. 112, no. 2, 309-324.

Kinsman, D.J.J., and H.D. Holland. 1969. "The Co-precipitation of Cations with $CaCO_3$-IV. The Co-precipitation of Sr^{2+} with Aragonite between 16° and 96°C," *Geochimica et Cosmochimica Acta.* Vol. 33, no. 1, 1-17.

Kitano, Y., N. Kanamori, and R. Fujiyoshi. 1978. "Distribution of Cadmium between Calcium Carbonate and Solution. Part 2. '$Ca(HCO_3)$ + Cd^{2+} + NaCl--> Carbonate' System," *Geochemical Journal.* Vol. 12, no. 3, 147-151.

Königsberger, E., R. Hausner, and H. Gamsjäger. 1991. "Solid-Solute Phase Equilibria in Aqueous Solution. V: The System $CdCO_3$-$CaCO_3$-CO_2-H_2O," *Geochimica et Cosmochimica Acta.* Vol. 55, no. 12, 3505-3514

Lahann, R.W., and R.M. Siebert. 1982. "A Kinetic Model for Distribution Coefficients and Application to Mg-calcites," *Geochimica et Cosmochimica Acta.* Vol. 46, no. 11, 2229-2237.

Morse, J.W. 1986. "The Surface Chemistry of Calcium Carbonate Minerals in Natural Waters: An Overview," *Marine Chemistry.* Vol. 20, no. 1, 91-112.

Mucci, A., and J.W. Morse. 1983. "The Incorporation of Mg^{2+} and Sr^{2+} into Calcite Overgrowths: Influences of Growth Rate and Solution Composition," *Geochimica et Cosmochimica Acta.* Vol. 47, no. 1, 217-233.

Mucci, A., and J.W. Morse. 1985. "Auger Spectroscopy Determination of the Surface-Most Adsorbed Layer Composition on Aragonite, Calcite, Dolomite, and Magnesite in Synthetic Seawater," *American Journal of Science.* Vol. 285, no. 4, 306-317.

Nyffeler, U.P., Y-H. Li, and P.H. Santschi. 1984. "A Kinetic Approach to Describe Trace-Element Distribution between Particles and Solution in Natural Aquatic Systems," *Geochimica et Cosmochimica Acta.* Vol. 48, no. 7, 1513-1522.

Perry, D.L. 1986. "Applications of Surface Techniques to Chemical Bonding Studies of Minerals," *Geochemical Processes at Mineral Surfaces, Chicago, IL, September 8-13, 1985.* Eds. J.A. Davis and K.F. Hayes. ACS Symposium Series 323. Washington, DC: American Chemical Society. 389-402.

Pingitore, N.E., Jr., and M.P. Eastman. 1984. "The Experimental Partitioning of Ba^{2+} into Calcite," *Chemical Geology.* Vol. 45, no. 1/2, 113-120.

Pingitore, N.E., Jr., and M.P. Eastman. 1986. "The Coprecipitation of Sr^{2+} with Calcite at 25°C and 1 Atm," *Geochimica et Cosmochimica Acta.* Vol. 50, no. 10, 2195-2203.

Pingitore, N.E., Jr., M.P. Eastman, M. Sandidge, K. Oden, and B. Freiha. 1988. "The Coprecipitation of Manganese(II) with Calcite: An Experimental Study," *Marine Chemistry.* Vol. 25, no. 2, 107-120.

Pingitore, N.E., Jr., F.W. Lytle, B.M. Davies, M.P. Eastman, P.G. Eller, and E.M. Larson. 1992. "Mode of Incorporation of Sr^{2+} in Calcite: Determination by X-ray Absorption Spectroscopy," *Geochimica et Cosmochimica Acta.* Vol. 56, no. 4, 1531-1538

Sposito, G. 1986. "Distinguishing Adsorption from Surface Precipitation," *Geochemical Processes at Mineral Surfaces, Chicago, IL, September 8-13, 1985.* Eds. J.A. Davis and K.F. Hayes. ACS Symposium Series 323. Washington, DC: American Chemical Society. 217-228.

Stipp, S.L., and M.F. Hochella, Jr. 1991. "Structure and Bonding Environments at the Calcite Surface as Observed with X-ray Photoelectron Spectroscopy (XPS) and Low Energy Electron Diffraction (LEED)," *Geochimica et Cosmochimica Acta.* Vol. 55, no. 6, 1723-1736.

Terakado, Y., and A. Masuda. 1988. "The Coprecipitation of Rare-Earth Elements with Calcite and Aragonite," *Chemical Geology.* Vol. 69, no. 1, 103-110.

Thorstenson, D.C., and L.N. Plummer. 1977. "Equilibrium Criteria for Two-component Solids Reacting with Fixed Composition in an Aqueous Phase--Example: The Magnesian Calcites," *American Journal of Science.* Vol. 277, no. 9, 1203-1223.

Van Luik, A.E., and J.J. Jurinak. 1979. "Equilibrium Chemistry of Heavy Metals in Concentrated Electrolyte Solution," *Chemical Modeling in Aqueous Systems: Speciation, Sorption, Solubility, and Kinetics Miami Beach, FL, September 11-13, 1978.* Ed. E.A. Jenne. ACS Symposium Series 93. Washington, DC: American Chemical Society. 683-710.

Vuceta, J., and J.J. Morgan. 1978. "Chemical Modeling of Trace Metals in Fresh Waters: Role of Complexation and Adsorption," *Environmental Science and Technology.* Vol. 12, no. 12, 1302-1309.

DISTRIBUTION

Federal Agencies

US Department of Energy (6)
Office of Civilian Radioactive Waste Management
Attn: Deputy Director, RW-2
Associate Director, RW-10/50
Office of Program and Resources Management
Office of Contract Business Management
Director, RW-22
Analysis and Verification Division
Associate Director, RW-30
Office of Systems and Compliance
Associate Director, RW-40
Office of Storage and Transportation
Director, RW-4/5
Office of Strategic Planning and International Programs
Office of External Relations
Forrestal Building
Washington, DC 20585

US Department of Energy
Albuquerque Operations Office
Attn: National Atomic Museum Library
PO Box 5400
Albuquerque, NM 87185-5400

US Department of Energy (4)
WIPP Project Integration Office
Attn: W.J. Arthur III
L.W. Gage
P.J. Higgins
D.A. Olona
PO Box 5400
Albuquerque, NM 87115-5400

US Department of Energy (2)
WIPP Project Integration Satellite Office
Attn: R. Batra
R. Becker
PO Box 3090, Mail Stop 525
Carlsbad, NM 88221-3090

US Department of Energy
Research & Waste Management Division
Attn: Director
PO Box E
Oak Ridge, TN 37831

US Department of Energy (3)
WIPP Project Site Office (Carlsbad)
Attn: V. Daub
J. Lippis
J.A. Mewhinney
PO Box 3090
Carlsbad, NM 88221-3090

US Department of Energy
Attn: E. Young
Room E-178
GAO/RCED/GTN
Washington, DC 20545

US Department of Energy
Office of Environmental Restoration and Waste Management
Attn: J. Lytle, EM-30,
Trevion II
Washington, DC 20585-0002

US Department of Energy (3)
Office of Environmental Restoration and Waste Management
Attn: M. Frei, EM-34,
Trevion II
Washington, DC 20585-0002

US Department of Energy
Office of Environmental Restoration and Waste Management
Attn: S. Schneider, EM-342,
Trevion II
Washington, DC 20585-0002

US Department of Energy (2)
Office of Environment, Safety and Health
Attn: C. Borgstrom, EH-25
R. Pelletier, EH-231
Washington, DC 20585

US Department of Energy (2)
Idaho Operations Office
Fuel Processing and Waste Management Division
785 DOE Place
Idaho Falls, ID 83402

US Environmental Protection Agency (2)
Radiation Protection Programs
Attn: M. Oge
ANR-460
Washington, DC 20460

US Geological Survey (2)
Water Resources Division
Attn: R. Livingston
4501 Indian School NE
Suite 200
Albuquerque, NM 87110

US Nuclear Regulatory Commission
Division of Waste Management
Attn: H. Marson
Mail Stop 4-H-3
Washington, DC 20555

Boards

Defense Nuclear Facilities Safety Board
Attn: D. Winters
625 Indiana Ave. NW, Suite 700
Washington, DC 20004

Nuclear Waste Technical Review Board (2)
Attn: Chairman
S.J.S. Parry
1100 Wilson Blvd., Suite 910
Arlington, VA 22209-2297

Advisory Committee on Nuclear Waste
Nuclear Regulatory Commission
Attn: R. Major
7920 Norfolk Ave.
Bethesda, MD 20814

State Agencies

Environmental Evaluation Group (3)
Attn: Library
7007 Wyoming NE
Suite F-2
Albuquerque, NM 87109

NM Bureau of Mines and Mineral Resources
Socorro, NM 87801

NM Energy, Minerals, and Natural Resources Department
Attn: Library
2040 S. Pacheco
Santa Fe, NM 87505

NM Environment Department (3)
Secretary of the Environment
Attn: J. Espinosa
1190 St. Francis Drive
Santa Fe, NM 87503-0968

NM Environment Department
WIPP Project Site
Attn: P. McCasland
PO Box 3090
Carlsbad, NM 88221

Laboratories/Corporations

Battelle Pacific Northwest Laboratories
Attn: R.E. Westerman, MSIN P8-44
Battelle Blvd.
Richland, WA 99352

INTERA Inc.
Attn: J.F. Pickens
6850 Austin Center Blvd., Suite 300
Austin, TX 78731

INTERA Inc.
Attn: W. Stensrud
PO Box 2123
Carlsbad, NM 88221

IT Corporation
Attn: R.F. McKinney
Regional Office
5301 Central NE, Suite 700
Albuquerque, NM 87108

Lawrence Livermore National Laboratory (15)
Attn: S.A. Carroll
Earth Sciences Department
Livermore, CA 94550

Los Alamos National Laboratory
Attn: B. Erdal, INC-12
PO Box 1663
Los Alamos, NM 87544

RE/SPEC, Inc.
Attn: W. Coons
4775 Indian School NE
Suite 300
Albuquerque, NM 87110-3927

RE/SPEC, Inc.
Attn: J.L. Ratigan
PO Box 725
Rapid City, SD 57709

Southwest Research Institute (2)
Center for Nuclear Waste Regulatory Analysis
Attn: P.K. Nair
6220 Culebra Road
San Antonio, TX 78228-0510

SAIC
Attn: D.C. Royer
101 Convention Center Dr.
Las Vegas, NV 89109

SAIC
Attn: H.R. Pratt
10260 Campus Point Dr.
San Diego, CA 92121

SAIC (2)
Attn: M. Davis
J. Tollison
2109 Air Park Rd. SE
Albuquerque, NM 87106

Tech Reps Inc. (3)
Attn: J. Chapman
C. Crawford
T. Peterson
5000 Marble NE, Suite 222
Albuquerque, NM 87110

TRW Environmental Safety Systems
Attn: L. Wildman
2650 Park Tower Dr., Suite 1300
Vienna, VA 22180-7306

Westinghouse Electric Corporation (5)
Attn: Library
C. Cox
L. Fitch
B.A. Howard
R. Kehrman
PO Box 2078
Carlsbad, NM 88221

Westinghouse-Savannah River
Technology Center (4)
Attn: N. Bibler
J.R. Harbour
M.J. Plodinec
G.G. Wicks
Aiken, SC 29802

National Academy of Sciences, WIPP Panel

Howard Adler
Oak Ridge Associated Universities
Medical Sciences Division
PO Box 117
Oak Ridge, TN 37831-0117

Fred M. Ernsberger
250 Old Mill Road
Pittsburgh, PA 15238

Ina Alterman
Board on Radioactive
Waste Management, GF456
2101 Constitution Ave.
Washington, DC 20418

John D. Bredehoeft
Western Region Hydrologist
Water Resources Division
US Geological Survey (M/S 439)
345 Middlefield Road
Menlo Park, CA 94025

Rodney C. Ewing
Department of Geology
University of New Mexico
Albuquerque, NM 87131

Charles Fairhurst, Chairman
Department of Civil and
Mineral Engineering
University of Minnesota
500 Pillsbury Dr. SE
Minneapolis, MN 55455-0220

B. John Garrick
PLG Incorporated
4590 MacArthur Blvd.
Suite 400
Newport Beach, CA 92660-2027

Leonard F. Konikow
US Geological Survey
431 National Center
Reston, VA 22092

Carl A. Anderson, Director
Board on Radioactive Waste Management
National Research Council
HA 456
2101 Constitution Ave. NW
Washington, DC 20418

Jeremiah O'Driscoll
Jody Incorporated
505 Valley Hill Drive
Atlanta, GA 30350

Christopher G. Whipple
Clement International
160 Spear St.
Suite 1380
San Francisco, CA 94105

Individuals

P. Drez
8816 Cherry Hills Rd. NE
Albuquerque, NM 87111

D.W. Powers
Star Route Box 87
Anthony, TX 79821

Universities

University of Missouri-Columbia (15)
Attn: D.L. Stout
Department of Geological Sciences
Columbia, MO 65211

University of New Mexico
Geology Department
Attn: Library
Albuquerque, NM 87131

University of Washington
College of Ocean
and Fishery Sciences
Attn: G.R. Heath
583 Henderson Hall
Seattle, WA 98195

Libraries

Thomas Brannigan Library
Attn: D. Dresp
106 W. Hadley St.
Las Cruces, NM 88001

Government Publications Department
Zimmerman Library
University of New Mexico
Albuquerque, NM 87131

New Mexico Junior College
Pannell Library
Attn: R. Hill
Lovington Highway
Hobbs, NM 88240

New Mexico State Library
Attn: N. McCallan
325 Don Gaspar
Santa Fe, NM 87503

New Mexico Tech
Martin Speere Memorial Library
Campus Street
Socorro, NM 87810

WIPP Public Reading Room
Carlsbad Public Library
Attn: Director
101 S. Halagueno St.
Carlsbad, NM 88220

Foreign Addresses

Studiecentrum Voor Kernenergie
Centre D'Energie Nucleaire
Attn: A. Bonne
SCK/CEN Boeretang 200
B-2400 Mol, BELGIUM

Atomic Energy of Canada, Ltd. (3)
Whiteshell Research Laboratories
Attn: B. Goodwin
M. Stevens
D. Wushke
Pinewa, Manitoba, CANADA ROE 1LO

Francois Chenevier (2)
ANDRA
Route du Panorama Robert Schumann
B.P. 38
92266 Fontenay-aux-Roses, Cedex
FRANCE

Jean-Pierre Olivier
OECD Nuclear Energy Agency
Division of Radiation Protection
and Waste Management
38, Boulevard Suchet
75016 Paris, FRANCE

Claude Sombret
Centre D'Études Nucléaires
De La Vallee Rhone
CEN/VALRHO
S.D.H.A. B.P. 171
30205 Bagnols-Sur-Ceze
FRANCE

Gesellschaft fur Reaktorsicherheit
(GRS) (2)
Attn: B. Baltes
W. Muller
Schwertnergasse 1
D-5000 Cologne, GERMANY

Bundesanstalt fur Geowissenschaften
und Rohstoffe
Attn: M. Langer
Postfach 510 153
3000 Hanover 51, GERMANY

Bundesministerium fur Forschung und
Technologie
Postfach 200 706
5300 Bonn 2, GERMANY

Institut fur Tieflagerung (2)
Attn: K. Kuhn
Theodor-Heuss-Strasse 4
D-3300 Braunschweig, GERMANY

Physikalisch-Technische Bundesanstalt
Attn: P. Brenneke
Postfach 3345
D-3300 Braunschweig, GERMANY

Shingo Tashiro
Japan Atomic Energy Research Inst.
Tokai-Mura, Ibaraki-Ken, 319-11
JAPAN

Netherlands Energy Research
Foundation ECN
Attn: L.H. Vons
3 Westerduinweg
PO Box 1
1755 ZG Petten, THE NETHERLANDS

Svensk Kärnbränsleforsorjning AB
Attn: F. Karlsson
Project KBS
Kärnbränslesakerhet
Box 5864
10248 Stockholm, SWEDEN

Nationale Genossenschaft für die
Lagerung radioaktiver Abfälle (2)
Attn: S. Vomvoris
P. Zuidema
Hardstrasse 73
CH-5430 Wettingen, SWITZERLAND

AEA Technology
Attn: J.H. Rees
D5W/29 Culham Laboratory
Abington, Oxfordshire OX14 3DB
UNITED KINGDOM

AEA Technology
Attn: W.R. Rodwell
044/A31 Winfrith Technical Centre
Dorchester, Dorset DT2 8DH
UNITED KINGDOM

AEA Technology
Attn: J.E. Tinson
B4244 Harwell Laboratory
Didcot, Oxfordshire OX11 ORA
UNITED KINGDOM

D.R. Knowles
British Nuclear Fuels, plc
Risley, Warrington, Cheshire WA3 6AS
1002607 UNITED KINGDOM

Internal

1502	J.C. Cummings
4511	D.P. Garber
6000	D.L. Hartley
6115	P.B. Davies
6115	Staff (15)
6119	F. Gelbard
6119	C.F. Novak (15)
6119	Staff (7)
6121	J.R. Tillerson
6121	Staff (7)
6300	D.E. Ellis
6302	L.E. Shephard
6303	S.Y. Pickering
6303	W.D. Weart
6305	S.A. Goldstein
6305	A.R. Lappin
6306	A.L. Stevens
6342	D.R. Anderson
6342	Staff (20)
6343	V. Harper-Slaboszewicz
6343	Staff (2)
6345	R.C. Lincoln
6345	Staff (9)
6347	D.R. Schafer
6348	J.T. Holmes
6348	Staff (4)
6351	R.E. Thompson
6352	S.E. Sharpton
6352	WIPP Central Files (10)
7141	Technical Library (5)
7151	Technical Publications
7613-2	Document Processing for DOE/OSTI (10)
8523-2	Central Technical Files

* U.S. GOVERNMENT PRINTING OFFICE 1993—774-122/80258

DATE
FILMED
1/11/94
END